Medicinal Chemistry Research
https://doi.org/10.1007/s00044-018-2141-9

MEDICINAL CHEMISTRY RESEARCH

ORIGINAL RESEARCH

Design, synthesis, evaluation and molecular modeling studies of some novel *N*-substituted piperidine-3-carboxylic acid derivatives as potential anticonvulsants

Ankit Seth[1] · Piyoosh A. Sharma[1] · Avanish Tripathi[1] · Priyanka K. Choubey[1] · Pavan Srivastava[1] · Prabhash Nath Tripathi[1] · Sushant Kumar Shrivastava[1]

Received: 25 September 2017 / Accepted: 20 January 2018

Abstract

Novel Schiff bases of 1-(2-Aminoethyl)piperidine-3-carboxylic acid were synthesized, characterized and screened for anticonvulsant activity. Compounds were evaluated for in vitro blood–brain barrier (BBB) permeability by parallel artificial membrane permeability BBB assay (PAMPA-BBB). Compounds **5d**, **5f**, **5j**, **5l**, **5m**, **5n**, **5w**, **5x** and **5y** elicited considerable in vitro permeability across BBB and further screened for in vivo anticonvulsant activity by sc-PTZ and DMCM-induced seizure models. The outcome of the in vivo models suggested that **5d, 5w**, and **5y** were most potent amongst the synthesized compounds. The neurotoxicity evaluation of **5d, 5w**, and **5y** by rotarod indicates no impairment of muscle coordination in comparison to standard diazepam. The MTT assay revealed that the test compounds (**5d, 5w**, and **5y**) were not found to alter the cell viability considerably. In silico molecular docking and dynamics simulations were carried out on the homology modeled protein of human GABA transporter 1 (GAT1), which exhibited complementary interactions of compound **5w** within the active binding pocket.

Keywords Schiff bases · Anti-convulsant · Piperidine-3-carboxylic acid · PAMPA-BBB · Rota rod test · MTT assay

Introduction

Epilepsy is a complex set of neurological disorders (Villalba et al. 2016), which is mainly characterized by unpredictable and frequent disturbances of normal brain function in the form of convulsive seizure episodes and/or loss of consciousness (Siddiqui et al. 2017). Despite the availability of numerous antiepileptic agents in the drug market, nearly 20–30% of the 70 million epilepsy patients worldwide have insufficient control over seizures and are resistant to the currently available pharmacotherapy (Ghareb et al. 2017). Moreover, the poor tolerability and reported side effects of the antiepileptic drugs have affected the quality of life of the epilepsy patients (El-Helby et al. 2017). Thus, to address these massive challenges, development of novel antiepileptic drugs with improved efficacy, considerable tolerability, and lower toxicity is a paramount necessity.

GABA is the main inhibitory neurotransmitter in the brain of mammals that plays a considerable role in the pathogenesis of epilepsy (Holmes 1995). Low brain GABA concentration and diminution in GABA-ergic neurotransmission have been observed in a range of epileptic syndromes (Petroff et al. 1996). The transport of GABA from synaptic cleft to the glial cells as well as presynaptic neurons is mediated by GABA transporters (GATs), which results in the termination of GABA-ergic neurotransmission. GATs are the member of sodium symporters, which belong to solute carrier 6 (SLC6) transporter gene family in humans that mediates neurotransmitter transport (Chen et al. 2004). Elevation in GABA concentration within the synaptic cleft is proved to be advantageous in the management of epilepsy. One such strategy for the up-regulation of GABA would be the blockade of specific

Electronic supplementary material The online version of this article (https://doi.org/10.1007/s00044-018-2141-9) contains supplementary material, which is available to authorized users.

✉ Sushant Kumar Shrivastava
skshrivastava.phe@iitbhu.ac.in

[1] Pharmaceutical Chemistry Research Laboratory, Department of Pharmaceutical Engineering & Technology, Indian Institute of Technology (Banaras Hindu University), Varanasi 221005, India

Published online: 06 February 2018

subtypes of GATs, which are responsible for neuronal and glial uptake of GABA from the synaptic cleft (Quandt et al. 2013). Inhibitors of GABA uptake are of utmost significance as regulators of neurotransmitter levels that increase the duration of inhibitory postsynaptic potentials to elicit antiepileptic activity (Thompson and Gahwiler 1992; Suzdak and Jansen 1995).

The discovery of piperidine-3-carboxylic acid (nipecotic acid) as a high-affinity substrate for GABA transporter remarkably added new prospects of targeting GABA uptake systems. It has been reported to exhibit significant in vitro activity as an inhibitor of uptake of GABA into neuronal and glial cells (Krogsgaard-Larsen 1980). However, it is unable to cross BBB owing to its zwitterionic and polar nature (Andersen et al. 2001a). The synthetic versatility of piperidine-3-carboxylic acid led to the discovery of lipophilic derivatives which have been explored as useful inhibitors of GABA uptake. Initially, N-(4,4-diphenyl-3-butenyl)-nipecotic acid (SK&F 89976 A) (Yunger et al. 1984; Löscher 1985; Ali et al. 1985), and NO-328 (tiagabine) (Nielsen et al. 1991; Braestrup et al. 1990), 1-(2-(bis (4-(trifluoromethyl)phenyl)methoxy)ethyl)-1,2,5,6-tetrahydropyridine-3-carboxylic acid, (Cl966) (Bjorge et al. 1990; Taylor et al. 1990) (S)-1-(2-(tris(4-methoxyphenyl) methoxy)ethyl)piperidine-3-carboxylic acid (SNAP-5114) (Dhar et al. 1994) (Fig. 1) and N-(mono)-(diaryl methoxy) alkyl or N-(diaryl methoxy)alkyl derivatives (Falch and Krogsgaard-Larsen 1989) have demonstrated considerable in vitro GABA uptake inhibition thereby translating into effective anticonvulsants in some in vivo models. The findings have led to further exploration of the piperidine-3-carboxylic acid, resulting in the discovery of N-(benzhydryl ethyl ether) derivatives (Pavia et al. 1992), N-alkylene, alkyl or cycloalkylene derivatives (Andersen et al. 2001a), N-tricyclic derivatives (Andersen et al. 2001b), as in vitro inhibitors of GABA uptake with some leads demonstrating in vivo anticonvulsant activity. Despite the synthesis of these diverse derivatives, BBB permeation remains the key bottleneck for brain drug delivery. The single marketed derivative of the piperidine-3-carboxylic acid, i.e., tiagabine is a GAT-1 selective GABA uptake inhibitor with considerable antiepileptic potential. Reported GABA uptake inhibition triggered by tiagabine has been attributed to the presence of GABA mimetic moiety in the form of piperidine-3-carboxylic acid and a lipophilic di-aromatic region connected by a linker (Jurik et al. 2013). Tiagabine is effectively used as adjunctive therapy for the management of complex partial seizures in epilepsy patients (Prescott 1997). However, its long-term use is associated with adverse effects like asthenia, tremor, concentration difficulties, lethargy, nervousness, and depression (Ortinski and Meador 2004; Sveinbjornsdottir et al. 1994; Kälviäinen 2001). Therefore, scope to develop novel compounds with improved BBB permeation and lesser side effects is still a challenge for medicinal chemists in the discovery of new drugs to treat epilepsy.

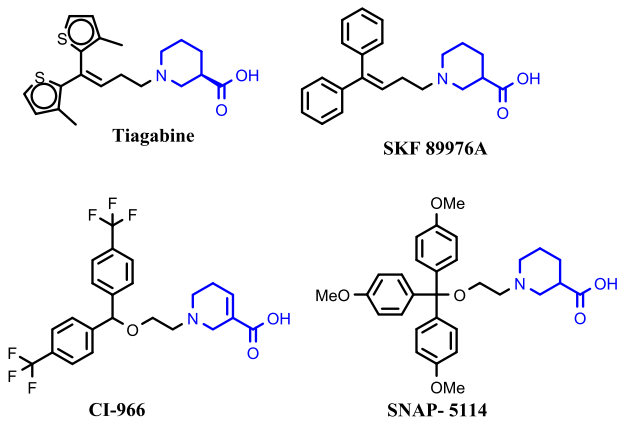

Fig. 1 Derivatives of piperidine-3-carboxylic acid as GABA uptake inhibitors

Schiff bases are reported to be attractive scaffolds in the exploration of new chemical entities as antiepileptics, owing to their lipophilic nature and reported applications in the design and synthesis of derivatives with marked antiepileptic activity (Pandeya and Rajput 2012; Swathi and Sarangapani 2015; Bhat and Al-Omar 2011; Kulkarni et al. 2017; Aly et al. 2010). These are the condensation products of primary amines with aldehydes or ketones. In the current work, Schiff bases have been synthesized by the reaction of 1-(2-aminoethyl)piperidine-3-carboxylic acid with corresponding aromatic aldehydes under acidic condition to obtain novel compounds with improved lipophilicity as compared to the parent scaffold. The synthesized compounds have been evaluated for their ability to permeate the blood–brain barrier (BBB) by an in vitro parallel artificial membrane permeability BBB assay (PAMPA-BBB). The potential leads exhibiting in vitro BBB permeability were further evaluated for anticonvulsant activity in *sc*-Pentylenetetrazole (PTZ) (Subcutaneous pentylenetetrazol) and DMCM (Methyl-6,7-dimethoxy-4-ethyl-β-carboline-3-carboxylate) induced seizure models. Neurological side effects of antiepileptic drugs have been reported in several literatures. Therefore, the effects of the leads on motor coordination were evaluated by rota-rod test on rodents. Also, the effects of the most active compounds on cell viability was determined in neuroblastoma cell line (SH-SY5Y) by 3-(4,5-dimethylthiazol-2-yl)-2,5-diphenyltetrazolium bromide (MTT) assay. The leads were then subjected to molecular docking on a homology modeled protein to identify and compare the complementary interactions of the compounds with the amino acid residues of the active pocket. The binding modes of the most active compound were further probed using molecular dynamics simulation at the GAT1

active site. A mechanistic hypothesis based on the binding mode of the ligand was also proposed.

Designing consideration

In vivo modulation of specific GAT isoform to selectively block neuronal or glial GABA uptake represents a herculean challenge with currently available pharmacological tools. This is due to the inability of the compounds to cross highly selective BBB. This problem can be circumvented by developing lipophilic analogs of the existing scaffolds with proven in vitro GABA uptake inhibitory potential. One such scaffold is piperidine-3-carboxylic acid, which has gained attention owing to its synthetic versatility (Krogsgaard-Larsen and Johnston 1975). Tiagabine, a new generation antiepileptic drug and a well-known GABA uptake inhibitor is a marketed derivative of piperidine-3-carboxylic acid. Considering tiagabine as a benchmark and taking cognizance of structure-activity relationship of the reported *N*-substituted piperidine-3-carboxylic acid derivatives, an attempt was made to synthesize a series of novel Schiff bases of 1-(2-aminoethyl) piperidine-3-carboxylic acid. Presence of an ethylene bridge in title compounds provides the necessary flexibility to the overall structure. Thus, the objective of this study was to design and synthesize some novel nipecotic acid derivatives with increased lipophilicity and permeability across BBB.

Materials and methods

Chemistry

Analytical grade chemicals and solvents procured from Sigma-Aldrich (India), Merck (Germany) and SD fine Chemicals (India) were used for the synthesis. To determine the melting points, open capillary tubes were used on a Stuart Melting Point apparatus (SMP10). Thin layer chromatography was performed on a pre-coated Merck silica gel 60F254 aluminum sheets (Merck, Germany) to observe the progress of the reaction. TLC visualization was accomplished by using UV cabinet (254 nm) or iodine vapors. Experimental Log *P* values of the synthesized compounds were determined by shake flask method using Shimadzu UV/Visible spectrophotometer. FT-IR spectrophotometer (Shimadzu 8400S) was used to obtain the infrared spectrum of the intermediates and final compounds; analysis of the oil samples was done by their application in the form of films of fixed thickness while the solid samples were analyzed as KBr pellets. ^{1}H-NMR spectra (500 MHz) and ^{13}C-NMR (125 MHz) was recorded using Bruker Advance spectrophotometer using TMS as an internal standard. Exeter CE-440 Elemental Analyzer was used for elemental (C, H, and N) analyses and results obtained were within ±0.4% of the theoretical values.

General procedure for the synthesis of ethyl 1-(2-aminoethyl) piperidine-3-carboxylate (3)

Compound **3** was synthesized according to the reported procedure with slight modification (Murali Dhar et al. 1999). A mixture of ethyl nepicotate (7.76 mmol), K_2C0_3 (19.5 mmol) and KI (3.9 mmol) was dissolved in 1,4-dioxane with gentle heating. 2-Bromo ethylamine hydrobromide (16 mmol) was then added, and the reaction mixture was refluxed for 30 h. After completion, the reaction mixture was cooled to room temperature, and dioxane was evaporated under vacuum. The obtained residue was treated with ice-cold 3 N NaOH and further extracted with EtOAc (4 × 120 mL). The extracted organic layer was dried over (Na_2SO_4) and concentrated. The crude product was further purified by column chromatography on silica gel using DCM/methanol (9.5:0.5) as the mobile phase to afford the compound **3** as viscous brown oil.

FT-IR (KBr) ν_{max} 3366 (Asymmetric N–H), 3298 (Symmetric N–H), 2868 (C–H), 1748 (C=O). ^{1}H NMR (500 MHz, $CDCl_3$) $\delta = 4.21$ (2H, q, $J = 6.0$ Hz, $OC\underline{H}_2CH_3$), 3.25 (1H, dd, $J = 12.4$, 7.8 Hz, piperidine H-2a), 2.96–2.90 (1H, m, piperidine H-3), 2.88–2.65 (4H, m, H-1′, H-2′, $C{=}NCH_2$, NCH_2), 2.56 (1H, t, $J = 4.9$ Hz, piperidine H-6a), 2.52–2.41 (1H, m, piperidine H-4b), 2.38–2.26 (1H, m, piperidine H-6b, 2b), 1.91–1.64 (3H, m, piperidine H-4a, 5), 1.49 (1H, s, NH_2), 1.42 (3H, t, $J = 6.0$ Hz, $OCH_2C\underline{H}_3$). ^{13}C NMR (125 MHz, $CDCl_3$) $\delta = 173.9$ (C=O, $\underline{C}OOC_2H_5$), 61.7 (CH_2, $O\underline{C}H_2CH_3$), 60.8 (CH_2, C-1′), 56.8 (CH_2, piperidine C-2), 53.6 (CH_2, piperidine C-6), 44.6 (CH, piperidine C-3), 39.3 (CH_2, C-2′), 24.9 (CH_2, piperidine C-4), 22.6 (CH_2, piperidine C-5), 14.7(CH_3, $OCH_2\underline{C}H_3$). Anal. calcd. for $C_{10}H_{20}N_2O_2$**:** C, 59.97; H, 10.07; N, 13.99. Found: C, 59.82; H, 10.04; N, 13.95.

General procedure for the synthesis of 1-(2-aminoethyl) piperidine-3-carboxylic acid (4)

The synthesized compound **3** was hydrolyzed following the reported protocol with slight modification (Andersen et al. 2001a). The corresponding compound **2** (1.0 mmol) and 4 N NaOH solution (3.0 mmol) were taken in ethanol (3 mL). The reaction mixture was stirred at room temperature (3–6 h). Completion of the reaction was monitored by TLC using DCM/methanol (9.5:0.5). The reaction mixture was kept on an ice bath followed by the workup with 1 N HCl and then dried under vacuum to yield the compound **4**.

FT-IR (KBr) ν_{max} 3363 (Asymmetric N–H), 3304 (Symmetric N–H), 3212 (O–H), 2860 (C–H), 1724

(C=O).^{1}H NMR (500 MHz, $CDCl_3$) $\delta = 11.46$ (1H, s, COOH), 3.01 (1H, dd, $J = 12.4$, 7.6Hz, piperidine H-2a), 2.83–2.68 (5H, m, H-1′, H-2′, piperidine H-3, C=NCH_2, NCH_2), 2.56 (1H, t, $J = 4.9$ Hz, piperidine H-6a), 2.53–2.41 (1H, m, piperidine H-2b), 2.32–2.23 (1H, m, piperidine H-6b), 2.11 (1H, dd, $J = 14.0$, 6.1 Hz, piperidine H-4a), 1.77–1.59 (3H, m, piperidine H-4b, 5), 1.45 (2H, s, NH_2). ^{13}C NMR (125 MHz, $CDCl_3$) $\delta = 182.9$ (C=O, COOH), 67.4 (CH_2, C-1′), 62.0 (CH_2, piperidine C-2), 60.2 (CH_2, piperidine C-6), 47.5 (CH, piperidine C-3), 45.9 (CH_2, C-2′), 31.7 (CH_2, piperidine C-4), 29.2 (CH_2, piperidine C-5). Anal. calcd. for $C_8H_{16}N_2O_2$: C, 55.79; H, 9.36; N, 16.27. Found: C, 55.61; H, 9.34; N, 16.31.

General procedure for the synthesis of compounds (5a–5y)

Compound **4** (1 mmol) was dissolved in absolute ethanol (20 mL) with gentle heating, followed by addition of 2–3 drops of glacial acetic acid. Corresponding aromatic aldehydes (1.2 mmol) were added, and the reaction mixture was refluxed till the completion of reaction (3–5 h) as monitored by TLC using DCM/methanol (9.5:0.5) as the mobile phase. The obtained precipitate was filtered, dried and purified by column chromatography on silica gel with few drops of triethylamine using DCM/methanol as the mobile phase to yield the target compounds (**5a–5y**).

1-(2-(benzylideneamino)ethyl)piperidine-3-carboxylic acid (5a) Yield: 125 mg, 48.07%. FT-IR (KBr) ν_{max} 3220 (O–H), 3042 (Ar C–H), 2880 (C–H), 1712 (C=O), 1616 (C=N), 1586 (Ar C=C). ^{1}H NMR (500 MHz, $CDCl_3$) $\delta =$ 11.32 (s, 1H, COOH), 8.42 (s, 1H, H-3′, imine CH=N), 7.48–7.27 (m, 5H, phenyl H-2- H-6, Ar–H), 3.67 (2H, t, $J = 7.4$ Hz, H-2′, C=NCH_2), 3.04 (1H, dd, $J = 12.5$, 7.7 Hz, piperidine H-2a), 2.84 (2H, t, $J = 7.2$ Hz, H-1′, NCH_2), 2.78–2.67 (2H, m, piperidine H-2b, 6a), 2.63 (1H, m, piperidine H-6b), 2.32 (1H, m, piperidine H-3), 2.11 (1H, m, piperidine H-4a), 1.77–1.64 (3H, m, piperidine H-5, 4b). ^{13}C NMR (125 MHz, $CDCl_3$) $\delta = 181.2$ (C=O, COOH), 163.3 (imine CH, C-3′), 135.7 (C, Ar–C, phenyl C-1), 132.1 (CH, Ar–C, phenyl C-4), 128.8 (2 × CH, Ar–C, phenyl C-3, 5), 125.5 (2 × CH, Ar–C, phenyl C-2, 6), 63.1 (CH_2, C-1′), 59.8 (CH_2, C-2′), 59.5 (CH_2, piperidine C-2), 56.3 (CH_2, piperidine C-6), 49.1 (CH, piperidine C-3), 24.4 (CH_2, piperidine C-4), 20.4 (CH_2, piperidine C-5). Anal. calcd. for $C_{15}H_{20}N_2O_2$: C, 69.20; H, 7.74; N, 10.76. Found: C, 69.39; H, 7.76; N, 10.74.

1-(2-((2-chlorobenzylidene)amino)ethyl)piperidine-3-carboxylic acid (5b) Yield: 153 mg, 52.04%. FT-IR (KBr) ν_{max} 3236 (O–H), 3042 (Ar C–H), 2889 (C–H), 1716 (C=O), 1612 (C=N), 1585 (Ar C=C) 798 (C-Cl). ^{1}H NMR (500 MHz, $CDCl_3$) $\delta = 11.42$ (s, 1H, COOH), 8.32 (s, 1H, H-3′, imine CH=N), 7.44–7.22 (m, 4H, phenyl H-2- H-5, Ar–H), 3.58 (2H, t, $J = 7.1$ Hz, H-2′, C=NCH_2), 3.18 (1H, dd, $J = 12.3$, 7.7 Hz, piperidine H-2a), 2.71 (2H, t, $J = 7.1$ Hz, H-1′, NCH_2), 2.68–2.57 (2H, m, piperidine H-2b, 6a), 2.51–2.47 (1H, m, piperidine H-6b), 2.41–2.28 (1H, m, piperidine H-3), 2.08–2.04 (1H, m, piperidine H-4a), 1.76–1.59 (3H, m, piperidine H-5, 4b). ^{13}C NMR (125 MHz, $CDCl_3$) $\delta = 179.4$ (C=O, COOH), 161.9 (imine CH, C-3′), 136.4 (CH, Ar–C, phenyl C-6), 134.2 (C, Ar–C, phenyl C-1), 132.4 (CH, Ar–C, phenyl C-4), 130.7 (CH, Ar–C, phenyl C-5), 128.5 (CH, Ar–C, phenyl C-2), 124.3 (CH, Ar–C, phenyl C-3), 60.1 (CH_2, C-1′), 57.8 (CH_2, C-2′), 56.1 (CH_2, piperidine C-2), 55.7 (CH_2, piperidine C-6), 48.2 (CH, piperidine C-3), 24.6 (CH_2, piperidine C-4), 22.1 (CH_2, piperidine C-5). Anal. calcd. for $C_{15}H_{19}ClN_2O_2$: C, 61.12; H, 6.50; N, 9.50. Found: C, 61.03; H, 6.49; N, 9.52.

1-(2-((4-chlorobenzylidene)amino)ethyl)piperidine-3-carboxylic acid (5c) Yield: 133 mg, 45.24%. FT-IR (KBr) ν_{max} 3238 (O–H), 3041 (Ar C–H), 2878 (C–H), 1712 (C=O), 1614 (C=N), 1582 (Ar C=C) 812 (C-Cl).^{1}H NMR (500 MHz, $CDCl_3$) $\delta = 11.41$ (s, 1H, COOH), 8.28 (s, 1H, H-3′, imine CH=N), 7.51 (2H, d, $J = 7.5$ Hz, Ar–H, phenyl H-2, 6), 7.34 (2H, d, $J = 7.5$ Hz, Ar–H, phenyl H-3, 5), 3.66 (2H, t, $J = 4.9$ Hz, H-2′, C=NCH_2), 2.98 (1H, dd, $J = 12.4$, 7.8 Hz, piperidine H-2a), 2.76 (2H, t, $J = 4.9$ Hz, H-1′, NCH_2), 2.66–2.51 (2H, m, piperidine H-2b, 6a), 2.47–2.31 (1H, m, piperidine H-6b), 2.27–2.16 (1H, m, piperidine H-3), 2.09–1.95 (1H, m, piperidine H-4a), 1.68–1.47 (3H, m, piperidine H-5, 4b). ^{13}C NMR (125 MHz, $CDCl_3$) $\delta =$ 177.1 (C=O, COOH), 160.9 (imine CH, C-3′), 137.7 (C, Ar–C, phenyl C-4), 135.1 (CH, Ar–C, phenyl C-1), 129.7 (2 × CH, Ar–C, phenyl C-6, 2), 128.9 (2 × CH, Ar–C, phenyl C-5, 3), 60.1 (CH_2, C-1′), 58.8 (CH_2, C-2′), 57.5 (CH_2, piperidine C-2), 56.7 (CH_2, piperidine C-6), 55.1 (CH, piperidine C-3), 25.4 (CH_2, piperidine C-4), 21.4 (CH_2, piperidine C-5). Anal. calcd. for $C_{15}H_{19}ClN_2O_2$: C, 61.12; H, 6.50; N, 9.50. Found: C, 61.29; H, 6.52; N, 9.47.

1-(2-((2,3-dichlorobenzylidene)amino)ethyl)piperidine-3-carboxylic acid (5d) Yield: 168 mg, 51.22%. FT-IR (KBr) ν_{max} 3233 (O–H), 3041 (Ar C–H), 2876 (C–H), 1725 (C=O), 1617 (C=N), 1590 (Ar C=C) 797, 788 (C–Cl). ^{1}H NMR (500 MHz, $CDCl_3$) $\delta = 11.39$ (s, 1H, COOH), 8.77 (s, 1H, H-3′, imine CH=N), 7.58–7.20 (m, 3H, phenyl H-2- H-4, Ar–H), 4.00 (2H, t, $J = 4.8$ Hz, H-2′, C=NCH_2), 3.23 (1H, dd, $J = 12.3$, 7.7 Hz, piperidine H-2a), 3.05–2.96 (2H, m, H-1′, NCH_2), 2.86–2.79 (2H, m, piperidine H-2b, 6a), 2.65 (1H, dd, $J = 12.3$, 7.7 Hz, piperidine H-6b), 2.52–2.47 (1H, m, piperidine H-3), 2.37–2.31 (1H, m, piperidine H-4a), 1.92–1.83 (3H, m, piperidine H-5, 4b). ^{13}C NMR (125 MHz, $CDCl_3$) $\delta = 173.68$ (C=O, COOH), 160.7 (imine CH, C-3′), 132.4 (CH, Ar–C, phenyl C-1), 131.5 (C, Ar–C,

phenyl C-6), 131.1 (CH, Ar–C, phenyl C-4), 130.9 (CH, Ar–C, phenyl C-5), 125.5 (CH, Ar–C, phenyl C-3), 123.8 (CH, Ar–C, phenyl C-2), 56.8 (CH_2, C-1′), 52.7 (CH_2, C-2′), 52.6 (CH_2, piperidine C-2), 51.0 (CH_2, piperidine C-6), 38.2 (CH, piperidine C-3), 22.2 (CH_2, piperidine C-4), 19.9 (CH_2, piperidine C-5). Anal. calcd. for $C_{15}H_{18}Cl_2N_2O_2$: C, 54.72; H, 5.51; N, 8.51. Found: C, 54.89; H, 5.52; N, 8.50.

1-(2-((2,4-dichlorobenzylidene)amino)ethyl)piperidine-3-carboxylic acid (5e) Yield: 148 mg, 45.12%. FT-IR (KBr) ν_{max} 3230 (O–H), 3040 (Ar C–H), 2880 (C–H), 1718 (C=O), 1619 (C=N), 1591 (Ar C=C) 826, 798 (C–Cl). ^{1}H NMR (500 MHz, $CDCl_3$) $\delta = 11.51$ (s, 1H, COOH), 8.31 (s, 1H, H-3′, imine CH=N), 7.41–7.21 (m, 3H, phenyl H-2, 3, 4, Ar–H), 3.54 (2H, t, $J = 7.41$ Hz, H-2′, C=NCH_2), 3.18 (1H, dd, $J = 12.3$, 7.7 Hz, piperidine H-2a), 2.68 (2H, t, $J =$ 7.1 Hz, H-1′, NCH_2), 2.66–2.55 (2H, m, piperidine H-2b, 6a), 2.49 (1H, dd, $J = 12.3$, 7.7 Hz, piperidine H-6b), 2.40–2.0 (1H, m, piperidine H-3), 2.13–2.02 (1H, m, piperidine H-4a), 1.78–1.59 (3H, m, piperidine H-5, 4b). ^{13}C NMR (125 MHz, $CDCl_3$) $\delta = 178.4$ (C=O, COOH), 161.7 (imine CH, C-3′), 137.8 (C, Ar–C, phenyl C-4), 135.5 (C, Ar–C, phenyl C-6), 132.1 (C, Ar–C, phenyl C-1), 130.9 (C, Ar–C, phenyl C-5), 130.3 (C, Ar–C, phenyl C-2), 128.8 (C, Ar–C, phenyl C-3), 59.5 (CH_2, C-1′), 55.5 (CH_2, C-2′), 55.3 (CH_2, piperidine C-2), 53.7 (CH_2, piperidine C-6), 40.99 (CH, piperidine C-3), 24.2 (CH_2, piperidine C-4), 21.3 (CH_2, piperidine C-5). Anal. calcd. for $C_{15}H_{18}Cl_2N_2O_2$: C, 54.72; H, 5.51; N, 8.51. Found: C, 54.85; H, 5.53; N, 8.53.

1-(2-((2,3,6-trichlorobenzylidene)amino)ethyl)piperidine-3-carboxylic acid (5f) Yield: 172 mg, 47.51%. FT-IR (KBr) ν_{max} 3226 (O–H), 3066 (Ar C–H), 2871 (C–H), 1727 (C=O), 1611 (C=N), 1586 (Ar C=C) 811, 787, 778 (C-Cl). ^{1}H NMR (500 MHz, $CDCl_3$) $\delta = 11.21$ (s, 1H, COOH), 8.40 (s, 1H, H-3′, imine CH=N), 7.23–7.15 (m, 2H, phenyl H-3, 4, Ar–H), 3.50 (2H, t, $J = 5.1$ Hz, H-2′, C=NCH_2), 2.97 (1H, dd, $J = 12.3$, 7.7 Hz, piperidine H-2a), 2.33 (2H, t, $J = 7.1$ Hz, H-1′, NCH_2), 2.66–2.55 (2H, m, piperidine H-2b, 6a), 2.49 (1H, dd, $J = 12.3$, 7.7 Hz, piperidine H-6b), 2.35–2.30 (1H, m, piperidine H-3), 2.14–1.95 (1H, m, piperidine H-4a), 1.77–1.47 (3H, m, piperidine H-5, 4b). ^{13}C NMR (125 MHz, $CDCl_3$) $\delta = 174.4$ (C=O, COOH), 159.7 (imine CH, C-3′), 136.8 (C, Ar–C, phenyl C-1), 134.5 (C, Ar–C, phenyl C-6), 132.8 (C, Ar–C, phenyl C-4), 131.9 (C, Ar–C, phenyl C-2), 131.3 (C, Ar–C, phenyl C-5), 129.9 (C, Ar–C, phenyl C-3), 59.1 (CH_2, C-1′), 57.5 (CH_2, C-2′), 56.2 (CH_2, piperidine C-2), 54.1 (CH_2, piperidine C-6), 40.4 (CH, piperidine C-3), 25.2 (CH_2, piperidine C-4), 21.9 (CH_2, piperidine C-5). Anal. calcd. for $C_{15}H_{17}Cl_3N_2O_2$: C, 49.54; H, 4.71; N, 7.70. Found: C, 49.40; H, 4.70; N, 7.72.

1-(2-((3-fluorobenzylidene)amino)ethyl)piperidine-3-carboxylic acid (5g) Yield: 144 mg, 51.79%. FT-IR (KBr) ν_{max} 3229 (O–H), 3049 (Ar C–H), 2890 (C–H), 1721 (C=O), 1625 (C=N), 1594 (Ar C=C) 1278 (C–F). ^{1}H NMR (500 MHz, $CDCl_3$) $\delta = 11.51$ (s, 1H, COOH), 8.30 (s, 1H, H-3′, imine CH=N), 7.39–7.03 (m, 4H, phenyl H-2, 3, 4, 6, Ar–H), 3.70 (2H, t, $J = 5.0$ Hz, H-2′, C=NCH_2), 2.99 (1H, dd, $J = 12.4$, 7.6 Hz, piperidine H-2a), 2.77 (2H, t, $J =$ 5.0 Hz, H-1′, NCH_2), 2.68–2.54 (2H, m, piperidine H-2b, 6a), 2.46–2.29 (1H, m, piperidine H-6b), 2.23–2.19 (1H, m, piperidine H-3), 2.04–1.97 (1H, m, piperidine H-4a), 1.71–1.50 (3H, m, piperidine H-5, 4b). ^{13}C NMR (125 MHz, $CDCl_3$) $\delta = 177.4$ (C=O, COOH), 164.3 (d, $J_{C,F} =$ 259.4 Hz, C, Ar–C, phenyl C-5), 162.1 (d, $J_{C,F} = 4.5$ Hz, imine CH, C-3′), 139.8 (d, $J_{C,F} = 7.1$ Hz, C, Ar–C, phenyl C-1), 129.5 (d, $J_{C,F} = 7.1$ Hz, C, Ar–C, phenyl C-3), 124.8 (d, $J_{C,F} = 4.1$ Hz, C, Ar–C, phenyl C-2), 118.4 (d, $J_{C,F} =$ 26.2 Hz, C, Ar–C, phenyl C-4), 115.5 (d, $J_{C,F} = 27.3$ Hz, C, Ar–C, phenyl C-6), 59.4 (CH_2, C-1′), 55.5 (CH_2, C-2′), 55.1 (CH_2, piperidine C-2), 53.4 (CH_2, piperidine C-6), 40.7 (CH, piperidine C-3), 25.9 (CH_2, piperidine C-4), 22.9 (CH_2, piperidine C-5). Anal. calcd. for $C_{15}H_{19}FN_2O_2$: C, 64.73; H, 6.88; N, 10.07. Found: C, 64.94; H, 6.89; N, 10.03.

1-(2-((4-fluorobenzylidene)amino)ethyl)piperidine-3-carboxylic acid (5h) Yield: 122 mg, 43.88%. FT-IR (KBr) ν_{max} 3228 (O–H), 3039 (Ar C–H), 2887 (C–H), 1729 (C=O), 1620 (C=N), 1598 (Ar C=C) 1318 (C–F). ^{1}H NMR (500 MHz, $CDCl_3$) $\delta = 11.18$ (s, 1H, COOH), 8.27 (s, 1H, H-3′, imine CH=N), 7.64 (2H, d, $J = 7.5$ Hz, Ar–H, phenyl H-2, 6), 7.06 (2H, d, $J = 7.5$ Hz, Ar–H, phenyl H-3, 5), 3.59 (2H, t, $J = 5.3$ Hz, H-2′, C=NCH_2), 3.05 (1H, dd, $J = 12.3$, 7.7 Hz, piperidine H-2a), 2.90 (2H, t, $J = 5.3$ Hz, H-1′, NCH_2), 2.83–2.69 (2H, m, piperidine H-2b, 6a), 2.68–2.49 (1H, m, piperidine H-6b), 2.33–2.17 (1H, m, piperidine H-3), 2.16–1.91(1H, m, piperidine H-4a), 1.86–1.42 (3H, m, piperidine H-5, 4b). ^{13}C NMR (125 MHz, $CDCl_3$) $\delta = 176.4$ (C=O, COOH), 163.3 (d, $J_{C,F} =$ 248.8 Hz, C, Ar–C, phenyl C-4), 162.6 (imine CH, C-3′), 133.4 (d, $J_{C,F} = 3.8$ Hz, C, Ar–C, phenyl C-1), 131.7 (d, $J_{C,F} = 8.1$ Hz, 2 × CH, Ar–C, phenyl C-6, 2), 115.6 (d, $J_{C,F} =$ 24.8 Hz, 2 × CH, Ar–C, phenyl C-5, 3), 60.1 (CH_2, C-1′), 55.8 (CH_2, C-2′), 55.2 (CH_2, piperidine C-2), 53.7 (CH_2, piperidine C-6), 40.9 (CH, piperidine C-3), 25.9 (CH_2, piperidine C-4), 22.6 (CH_2, piperidine C-5). Anal. calcd. for $C_{15}H_{19}FN_2O_2$: C, 64.73; H, 6.88; N, 10.07. Found: C, 64.89; H, 6.86; N, 10.09.

1-(2-((2,4-difluorobenzylidene)amino)ethyl)piperidine-3-carboxylic acid (5i) Yield: 153 mg, 51.69%. FT-IR (KBr) ν_{max} 3242 (O–H), 3036 (Ar C–H), 2872 (C–H), 1716 (C=O), 1612 (C=N), 1588 (Ar C=C) 1319, 1292 (C–F).

^{1}H NMR (500 MHz, $CDCl_3$) $\delta = 11.21$ (s, 1H, COOH), 8.29 (s, 1H, H-3′, imine CH=N), 7.53–6.80 (m, 3H, phenyl H-2, 3, 4, Ar–H), 3.53 (2H, t, $J = 5.3$ Hz, H-2′, C=NCH_2), 3.06–2.81 (1H, m, piperidine H-2a), 2.74 (2H, t, $J = 7.1$ Hz, H-1′, NCH_2), 2.64–2.57 (2H, m, piperidine H-2b, 6a), 2.34–2.29 (1H, m, piperidine H-6b), 2.21–2.08 (1H, m, piperidine H-3), 2.05–1.99 (1H, m, piperidine H-4a), 1.72–1.61 (3H, m, piperidine H-5, 4b). ^{13}C NMR (125 MHz, $CDCl_3$) $\delta = 175.8$ (C=O, COOH), 165.3 (dd, $J_{C,F} =$ 190.1, 12.7 Hz, Ar–C–F, phenyl C-4), 163.4 (dd, $J_{C,F} =$ 188.3, 12.8 Hz, Ar–C–F, phenyl C-6), 160.6 (d, $J_{C,F} = 6.7$, imine CH, C-3′), 133.7 (dd, $J_{C,F} = 11.1$, 3.5 Hz, CH, Ar–C, phenyl C-2), 121.7 (dd, $J_{C,F} = 8.3$, 3.4 Hz, CH, Ar–C, phenyl C-1), 113.6 (dd, $J_{C,F} = 22.0$, 3.6 Hz, CH, Ar–C, phenyl C-3), 103.7 (t, $J_{C,F} = 24.9$ Hz, CH, Ar–C, phenyl C-5), 60.2 (CH_2, C-1′), 55.7 (CH_2, C-2′), 54.8 (CH_2, piperidine C-2), 53.8 (CH_2, piperidine C-6), 41.3 (CH, piperidine C-3), 24.9 (CH_2, piperidine C-4), 22.1 (CH_2, piperidine C-5). Anal. calcd. for $C_{15}H_{18}F_2N_2O_2$: C, 60.80; H, 6.12; N, 9.45. Found: C, 60.66; H, 6.11; N, 9.47.

1-(2-((3,4,5-trifluorobenzylidene)amino)ethyl)piperidine-3-carboxylic acid (5j) Yield: 168 mg, 53.50%. FT-IR (KBr) ν_{max} 3238 (O–H), 3038 (Ar C–H), 2868 (C–H), 1710 (C=O), 1616 (C=N), 1588 (Ar C=C) 1306, 1292, 1286 (C–F). ^{1}H NMR (500 MHz, $CDCl_3$) $\delta = 11.24$ (s, 1H, COOH), 8.29 (s, 1H, H-3′, imine CH=N), 7.10 (2H, dd, $J = 8.0$, 4.9 Hz, phenyl H-3, 4, Ar–H), 3.83 (2H, t, $J = 4.7$ Hz, H-2′, C=NCH_2), 3.47 (1H, dd, $J = 12.4$, 7.9 Hz, piperidine H-2a), 2.90 (2H, t, $J = 4.7$ Hz, H-1′, NCH_2), 2.77–2.54 (2H, m, piperidine H-2b, 6a), 2.26 (1H, dd, $J =$ 12.3, 7.7 Hz, piperidine H-6b), 2.18–2.11 (1H, m, piperidine H-3), 2.14–2.08 (1H, m, piperidine H-4a), 1.73–1.37 (3H, m, piperidine H-5, 4b). ^{13}C NMR (125 MHz, $CDCl_3$) $\delta = 174.4$ (C=O, COOH), 161.4 (t, $J_{C,F} = 4.1$ Hz, C, imine CH, C-3′), 149.8 (ddd, $J_{C,F} = 223.8$, 24.8, 7.2 Hz, C, Ar–C, phenyl C-5, 3), 140.5 (dt, $J_{C,F} = 49.8$, 28.2 Hz, C, Ar–C, phenyl C-4), 135.8 (td, $J_{C,F} = 5.9$, 3.9 Hz, C, Ar–C, phenyl C-1), 111.9 (ddd, $J_{C,F} = 27.9$, 7.2, 4.1 Hz, C, Ar–C, phenyl C-6, 2), 59.2 (CH_2, C-1′), 57.8 (CH_2, C-2′), 56.4 (CH_2, piperidine C-2), 54.6 (CH_2, piperidine C-6), 40.1 (CH, piperidine C-3), 25.8 (CH_2, piperidine C-4), 21.4 (CH_2, piperidine C-5). Anal. calcd. for $C_{15}H_{17}F_3N_2O_2$: C, 57.32; H, 5.45; N, 8.91. Found: C, 57.21; H, 5.47; N, 8.89.

1-(2-((3-bromobenzylidene)amino)ethyl)piperidine-3-carboxylic acid (5k) Yield: 166 mg, 49.11%. FT-IR (KBr) ν_{max} 3242 (O–H), 3028 (Ar C–H), 2868 (C–H), 1719 (C=O), 1622 (C=N), 1588 (Ar C=C), 628 (C-Br). ^{1}H NMR (500 MHz, $CDCl_3$) $\delta = 11.52$ (s, 1H, COOH), 8.28 (s, 1H, H-3′, imine CH=N), 7.90–7.19 (m, 4H, phenyl H-2- H-5, Ar–H), 3.59 (2H, t, $J = 6.2$ Hz, H-2′, C=NCH_2), 3.10 (1H, dd, $J = 12.2$, 7.7 Hz, piperidine H-2a), 2.81 (2H, t, $J =$ 6.2 Hz, H-1′, NCH_2), 2.74–2.70 (2H, m, piperidine H-2b, 6a), 2.52–2.48 (1H, m, piperidine H-6b), 2.34–2.29 (1H, m, piperidine H-3), 2.24–2.09 (1H, m, piperidine H-4a), 1.84–1.62 (3H, m, piperidine H-5, 4b). ^{13}C NMR (125 MHz, $CDCl_3$) $\delta = 176.5$ (C=O, COOH), 162.9 (imine CH, C-3′), 138.1 (CH, Ar–C, phenyl C-1), 134.3 (C, Ar–C, phenyl C-4), 131.4 (CH, Ar–C, phenyl C-6), 130.6 (CH, Ar–C, phenyl C-3), 126.5 (CH, Ar–C, phenyl C-2), 121.8 (CH, Ar–C, phenyl C-5), 69.2 (CH_2, C-1′), 57.9 (CH_2, C-2′), 56.2 (CH_2, piperidine C-2), 55.4 (CH_2, piperidine C-6), 47.3 (CH, piperidine C-3), 24.4 (CH_2, piperidine C-4), 21.9 (CH_2, piperidine C-5). Anal. calcd. for $C_{15}H_{19}BrN_2O_2$: C, 53.11; H, 5.65; N, 8.26. Found: C, 53.30; H, 5.65; N, 8.24.

1-(2-((4-bromobenzylidene)amino)ethyl)piperidine-3-carboxylic acid (5l) Yield: 143 mg, 42.31%. FT-IR (KBr) ν_{max} 3258 (O–H), 3053 (Ar C–H), 2898 (C–H), 1724 (C=O), 1619 (C=N), 1602 (Ar C=C), 639 (C–Br). ^{1}H NMR (500 MHz, $CDCl_3$) $\delta = 11.42$ (s, 1H, COOH), 8.26 (s, 1H, H-3′, imine CH=N), 7.49 (2H, d, $J = 7.5$ Hz, Ar–H, phenyl H-2, 6), 7.45 (2H, d, $J = 7.5$ Hz, Ar–H, phenyl H-3, 5), 3.57 (2H, t, $J = 5.3$ Hz, H-2′, C=NCH_2), 3.05 (1H, dd, $J = 12.5$, 7.7 Hz, piperidine H-2a), 2.90 (2H, t, $J = 5.3$ Hz, H-1′, NCH_2), 2.66–2.50 (2H, m, piperidine H-2b, 6a), 2.37 (1H, dd, $J =$ 12.5, 7.7 Hz, piperidine H-6b), 2.26–2.21 (1H, m, piperidine H-3), 2.15–1.96 (1H, m, piperidine H-4a), 1.74–1.54 (3H, m, piperidine H-5, 4b). ^{13}C NMR (125 MHz, $CDCl_3$) $\delta = 177.1$ (C=O, COOH), 160.9 (imine CH, C-3′), 137.7 (C, Ar–C, phenyl C-4), 135.1 (CH, Ar–C, phenyl C-1), 129.7 (2 × CH, Ar–C, phenyl C-6, 2), 128.9 (2 × C, Ar–C, phenyl C-5, 3), 60.1 (CH_2, C-1′), 58.8 (CH_2, C-2′), 57.5 (CH_2, piperidine C-2), 56.7 (CH_2, piperidine C-6), 55.1 (CH, piperidine C-3), 25.4 (CH_2, piperidine C-4), 21.4 (CH_2, piperidine C-5). Anal. calcd. for $C_{15}H_{19}BrN_2O_2$: C, 53.11; H, 5.65; N, 8.26. Found: C, 53.02; H, 5.64; N, 8.27.

1-(2-((2,6-dibromobenzylidene)amino)ethyl)piperidine-3-carboxylic acid (5m) Yield: 196 mg, 47.12%. FT-IR (KBr) ν_{max} 3255 (O–H), 3059 (Ar C–H), 2865 (C–H), 1718 (C=O), 1622 (C=N), 1598 (Ar C=C), 616 (C–Br). ^{1}H NMR (500 MHz, $CDCl_3$) $\delta = 11.51$ (s, 1H, COOH), 8.38 (s, 1H, H-3′, imine CH=N), 7.44–7.07 (m, 3H, phenyl H-2, 3, 4, Ar–H), 3.51 (2H, t, $J = 5.1$ Hz, H-2′, C=NCH_2), 3.05 (1H, dd, $J = 12.3$, 7.7 Hz, piperidine H-2a), 2.96 (2H, t, $J =$ 5.0 Hz, H-1′, NCH_2), 2.80–2.55 (2H, m, piperidine H-2b, 6a), 2.34 (1H, dd, $J = 12.4$, 7.8 Hz, piperidine H-6b), 2.31–2.25 (1H, m, piperidine H-3), 2.10–2.06 (1H, m, piperidine H-4a), 1.80–1.51 (3H, m, piperidine H-5, 4b). ^{13}C NMR (125 MHz, $CDCl_3$) $\delta = 173.4$ (C=O, COOH), 156.7 (imine CH, C-3′), 137.9 (C, Ar–C, phenyl C-1), 132.9 (2 × C, Ar–C, phenyl C-5, 3), 131.3 (C, Ar–C, phenyl C-4), 124.9 (2 × C, Ar–C, phenyl C-2, 6), 59.7 (CH_2, C-1′), 55.9 (CH_2, C-2′), 55.6 (CH_2, piperidine C-2), 54.7 (CH_2,

piperidine C-6), 40.1 (CH, piperidine C-3), 24.8 (CH_2, piperidine C-4), 22.6 (CH_2, piperidine C-5). Anal. calcd. for $C_{15}H_{18}Br_2N_2O_2$: C, 43.09; H, 4.34; N, 6.70. Found: C, 43.22; H, 4.35; N, 6.68.

1-(2-((4-nitrobenzylidene)amino)ethyl)piperidine-3-carboxylic acid (5n) Yield: 162 mg, 53.11%. FT-IR (KBr) ν_{max} 3233 (O–H), 3062 (Ar C–H), 2879 (C–H), 1706 (C=O), 1612 (C=N), 1596 (Ar C=C), 1562 (N=O). ^{1}H NMR (500 MHz, $CDCl_3$) $\delta = 11.28$ (s, 1H, COOH), 8.56 (s, 1H, H-3′, imine CH=N), 8.28 (2H, d, $J = 7.5$ Hz, Ar–H, phenyl H-2, 6), 8.11 (2H, d, $J = 7.5$ Hz, Ar–H, phenyl H-3, 5), 3.66 (2H, t, $J = 5.3$ Hz, H-2′, C=NCH_2), 2.95 (1H, dd, $J = 12.4$, 7.9 Hz, piperidine H-2a), 2.71 (2H, t, $J = 6.2$ Hz, H-1′, NCH_2), 2.64–2.47 (2H, m, piperidine H-2b, 6a), 2.39 (1H, dd, $J = 12.5$, 7.7 Hz, piperidine H-6b), 2.34–2.18 (1H, m, piperidine H-3), 2.14–1.92 (1H, m, piperidine H-4a), 1.87–1.32 (3H, m, piperidine H-5, 4b). ^{13}C NMR (125 MHz, $CDCl_3$) $\delta = 176.3$ (C=O, COOH), 161.2 (imine CH, C-3′), 151.1 (C, Ar–C, phenyl C-4), 140.5 (CH, Ar–C, phenyl C-1), 130.7 (2 × CH, Ar–C, phenyl C-6, 2), 124.6 (2 × C, Ar–C, phenyl C-5, 3), 61.3 (CH_2, C-1′), 57.2 (CH_2, C-2′), 55.5 (CH_2, piperidine C-2), 54.7 (CH_2, piperidine C-6), 41.1 (CH, piperidine C-3), 26.4 (CH_2, piperidine C-4), 21.8 (CH_2, piperidine C-5). Anal. calcd. for $C_{15}H_{19}N_3O_4$: C, 59.01; H, 6.27; N, 13.76. Found: C, 59.21; H, 6.25; N, 13.80.

1-(2-((2-nitrobenzylidene)amino)ethyl)piperidine-3-carboxylic acid (5o) Yield: 178 mg, 58.36%. FT-IR (KBr) ν_{max} 3242 (O–H), 3055 (Ar C–H), 2869 (C–H), 1721 (C=O), 1619 (C=N), 1585 (Ar C=C), 1545 (N=O). ^{1}H NMR (500 MHz, $CDCl_3$) $\delta = 11.42$ (s, 1H, COOH), 8.54 (s, 1H, H-3′, imine CH=N), 8.09–7.39 (m, 4H, phenyl H-2- H-5, Ar–H), 3.65 (2H, t, $J = 6.2$ Hz, H-2′, C=NCH_2), 2.98 (1H, dd, $J = 12.2$, 7.7 Hz, piperidine H-2a), 2.79 (2H, t, $J = 6.2$ Hz, H-1′, NCH_2), 2.68–2.63 (2H, m, piperidine H-2b, 6a), 2.57–2.41 (1H, m, piperidine H-6b), 2.37–2.24 (1H, m, piperidine H-3), 2.26–2.11 (1H, m, piperidine H-4a), 1.74–1.51 (3H, m, piperidine H-5, 4b). ^{13}C NMR (125 MHz, $CDCl_3$) $\delta = 172.9$ (C=O, COOH), 160.1 (imine CH, C-3′), 148.2 (CH, Ar–C, phenyl C-6), 133.7 (C, Ar–C, phenyl C-3), 132.6 (CH, Ar–C, phenyl C46), 131.7 (CH, Ar–C, phenyl C-2), 128.3 (CH, Ar–C, phenyl C-1), 124.9 (CH, Ar–C, phenyl C-5), 67.2 (CH_2, C-1′), 58.4 (CH_2, C-2′), 56.9 (CH_2, piperidine C-2), 55.2 (CH_2, piperidine C-6), 40.3 (CH, piperidine C-3), 24.1 (CH_2, piperidine C-4), 22.5 (CH_2, piperidine C-5). Anal. calcd. for $C_{15}H_{19}N_3O_4$: C, 59.01; H, 6.27; N, 13.76. Found: C, 59.18; H, 6.28; N, 13.73.

1-(2-((2-hydroxybenzylidene)amino)ethyl)piperidine-3-carboxylic acid (5p) Yield: 161 mg, 58.33%. FT-IR (KBr) ν_{max} 3368 (sharp, O–H), 3238 (broad, O–H), 3039 (Ar C–H), 2869 (C–H), 1717 (C=O), 1616 (C=N), 1588 (Ar C=C). ^{1}H NMR (500 MHz, $CDCl_3$) $\delta = 11.37$ (s, 1H, COOH), 9.02 (1H, s, Phenyl OH), 8.23 (s, 1H, H-3′, imine CH=N), 7.45–6.78 (m, 4H, phenyl H-2- H-5, Ar–H), 3.62 (2H, t, $J = 6.8$ Hz, H-2′, C=NCH_2), 3.22 (1H, dd, $J = 12.3$, 7.6 Hz, piperidine H-2a), 2.81 (2H, t, $J = 6.8$ Hz, H-1′, NCH_2), 2.75–2.61 (2H, m, piperidine H-2b, 6a), 2.66–2.54 (1H, m, piperidine H-6b), 2.39–2.32 (1H, m, piperidine H-3), 2.13–2.09 (1H, m, piperidine H-4a), 1.75–1.65 (3H, m, piperidine H-5, 4b). ^{13}C NMR (125 MHz, $CDCl_3$) $\delta = 176.4$ (C=O, COOH), 164.1 (imine CH, C-3′), 160.8 (CH, Ar–C, phenyl C-6), 133.1 (C, Ar–C, phenyl C-3), 129.3 (CH, Ar–C, phenyl C46), 121.7 (CH, Ar–C, phenyl C-2), 120.3 (CH, Ar–C, phenyl C-1), 117.9 (CH, Ar–C, phenyl C-5), 62.2 (CH_2, C-1′), 59.4 (CH_2, C-2′), 57.7 (CH_2, piperidine C-2), 55.7 (CH_2, piperidine C-6), 40.9 (CH, piperidine C-3), 24.4 (CH_2, piperidine C-4), 22.1 (CH_2, piperidine C-5). Anal. calcd. for $\mathbf{C_{15}H_{20}N_2O_3}$: C, 65.20; H, 7.30; N, 10.14. Found: C, 65.01; H, 7.28; N, 10.12.

1-(2-((4-hydroxybenzylidene)amino)ethyl)piperidine-3-carboxylic acid (5q) Yield: 146 mg, 52.89%. FT-IR (KBr) ν_{max} 3376 (sharp, O–H), 3239 (broad, O–H), 3068 (Ar C–H), 2862 (C–H), 1724 (C=O), 1628 (C=N), 1592 (Ar C=C). ^{1}H NMR (500 MHz, $CDCl_3$) $\delta = 11.28$ (s, 1H, COOH), 8.90 (1H, s, Phenyl OH), 8.25 (s, 1H, H-3′, imine CH=N), 7.40 (2H, d, $J = 7.5$ Hz, Ar–H, phenyl H-2, 6), 6.81 (2H, d, $J = 7.5$ Hz, Ar–H, phenyl H-3, 5), 3.69 (2H, t, $J = 5.0$ Hz, H-2′, C=NCH_2), 2.98 (1H, dd, $J = 12.3$, 7.7 Hz, piperidine H-2a), 2.77 (2H, t, $J = 5.0$ Hz, H-1′, NCH_2), 2.49–2.27 (2H, m, piperidine H-2b, 6a), 2.29 (1H, dd, $J = 12.5$, 7.7 Hz, piperidine H-6b), 2.10–1.93 (1H, m, piperidine H-3), 1.68–1.47 (1H, m, piperidine H-4a), 1.46–1.32 (3H, m, piperidine H-5, 4b). ^{13}C NMR (125 MHz, $CDCl_3$) $\delta = 176.4$ (C=O, COOH), 161.6 (imine CH, C-3′), 159.5 (C, Ar–C, phenyl C-4), 131.3 (2 × CH, Ar–C, phenyl C-6, 2), 127.5 (CH, Ar–C, phenyl C-1), 116.6 (2 × C, Ar–C, phenyl C-5, 3), 60.5 (CH_2, C-1′), 57.4 (CH_2, C-2′), 55.7 (CH_2, piperidine C-2), 52.9 (CH_2, piperidine C-6), 40.8 (CH, piperidine C-3), 23.4 (CH_2, piperidine C-4), 21.5 (CH_2, piperidine C-5). Anal. calcd. for $\mathbf{C_{15}H_{20}N_2O_3}$: C, 65.20; H, 7.30; N, 10.14. Found: C, 65.42; H, 7.31; N, 10.17.

1-(2-((3-methoxybenzylidene)amino)ethyl)piperidine-3-carboxylic acid (5r) Yield: 128 mg, 44.14 FT-IR (KBr) ν_{max} 3237 (O–H), 3049 (Ar C–H), 2885 (C–H), 1723 (C=O), 1618 (C=N), 1590 (Ar C=C). ^{1}H NMR (500 MHz, $CDCl_3$) $\delta = 11.21$ (s, 1H, COOH), 8.27 (s, 1H, H-3′, imine CH=N), 7.34-6.87 (m, 4H, phenyl H-2,4,5,6, Ar–H), 3.81 (3H, s, OCH_3), 3.72 (2H, t, $J = 5.4$ Hz, H-2′, C=NCH_2), 2.98 (1H, dd, $J = 12.3$, 7.7 Hz, piperidine H-2a), 2.84 (2H, t, $J = 5.4$

Hz, H-1′, NCH_2), 2.74–2.70 (2H, m, piperidine H-2b, 6a), 2.67–2.48 (1H, m, piperidine H-6b), 2.45–2.28 (1H, m, piperidine H-3), 2.20–2.08 (1H, m, piperidine H-4a), 1.79–1.56 (3H, m, piperidine H-5, 4b). ^{13}C NMR (125 MHz, $CDCl_3$) $\delta = 175.4$ (C=O, COOH), 162.7 (imine CH, C-3′), 160.1 (CH, Ar–C, phenyl C-1), 139.3 (C, Ar–C, phenyl C-4), 129.3 (CH, Ar–C, phenyl C-6), 122.6 (CH, Ar–C, phenyl C-3), 117.5 (CH, Ar–C, phenyl C-2), 112.1 (CH, Ar–C, phenyl C-5), 59.2 (CH_2, C-1′), 56.8 (CH_3, phenyl OCH_3), 55.9 (CH_2, C-2′), 55.2 (CH_2, piperidine C-2), 53.5 (CH_2, piperidine C-6), 40.8 (CH, piperidine C-3), 24.1 (CH_2, piperidine C-4), 22.3 (CH_2, piperidine C-5). Anal. calcd. for $\mathbf{C_{16}H_{22}N_2O_3}$: C, 66.18; H, 7.64; N, 9.65. Found: C, 66.40; H, 7.64; N, 9.63.

1-(2-((4-methoxybenzylidene)amino)ethyl)piperidine-3-carboxylic acid (5s) Yield: 122 mg, 42.06%. FT-IR (KBr) ν_{max} 3229 (O–H), 3040 (Ar C–H), 2875 (C–H), 1716 (C=O), 1622 (C=N), 1590 (Ar C=C). ^{1}H NMR (500 MHz, $CDCl_3$) $\delta = 11.36$ (s, 1H, COOH), 8.24 (s, 1H, H-3′, imine CH=N), 7.53 (2H, d, $J = 7.5$ Hz, Ar–H, phenyl H-2, 6), 6.93 (2H, d, $J = 7.5$ Hz, Ar–H, phenyl H-3, 5), 3.83 (3H, s, OCH_3), 3.68 (2H, t, $J = 4.9$ Hz, H-2′, C=NCH_2), 2.99 (1H, dd, $J = 12.5$, 7.7 Hz, piperidine H-2a), 2.76 (2H, t, $J = 4.9$ Hz, H-1′, NCH_2), 2.64–2.52 (2H, m, piperidine H-2b, 6a), 2.40 (1H, dd, $J = 12.5$, 7.7 Hz, piperidine H-6b), 2.24–2.15 (1H, m, piperidine H-3), 2.05–1.93 (1H, m, piperidine H-4a), 1.76–1.46 (3H, m, piperidine H-5, 4b). ^{13}C NMR (125 MHz, $CDCl_3$) $\delta = 175.4$ (C=O, COOH), 162.3 (C, Ar–C, phenyl C-4), 161.3 (imine CH, C-3′), 131.7 (2 × CH, Ar–C, phenyl C-6, 2), 128.4 (CH, Ar–C, phenyl C-1), 114.5 (2 × C, Ar–C, phenyl C-5, 3), 60.2 (CH_2, C-1′), 57.8 (CH_2, C-2′), 56.9 (CH_3, phenyl OCH_3), 55.2 (CH_2, piperidine C-2), 52.1 (CH_2, piperidine C-6), 40.9 (CH, piperidine C-3), 24.4 (CH_2, piperidine C-4), 22.8 (CH_2, piperidine C-5). Anal. calcd. for $C_{16}H_{22}N_2O_3$: C, 66.18; H, 7.64; N, 9.65. Found: C, 66.29; H, 7.66; N, 9.68.

1-(2-((3,4-dimethoxybenzylidene)amino)ethyl)piperidine-3-carboxylic acid (5t) Yield: 157 mg, 49.66%. FT-IR (KBr) ν_{max} 3228 (O–H), 3034 (Ar C–H), 2865 (C–H), 1716 (C=O), 1618 (C=N), 1585 (Ar C=C). ^{1}H NMR (500 MHz, $CDCl_3$) $\delta = 11.37$ (s, 1H, COOH), 8.19 (s, 1H, H-3′, imine CH=N), 7.26-6.89 (3H, phenyl H-2, 3, 6), 3.83 (3H, s, OCH_3), 3.81 (3H, s, OCH_3), 3.71 (2H, t, $J = 4.9$ Hz, H-2′, C=NCH_2), 2.97 (1H, dd, $J = 12.5$, 7.7 Hz, piperidine H-2a), 2.74 (2H, t, $J = 4.9$ Hz, H-1′, NCH_2), 2.63–2.54 (2H, m, piperidine H-2b, 6a), 2.38 (1H, dd, $J = 12.5$, 7.7 Hz, piperidine H-6b), 2.25–2.16 (1H, m, piperidine H-3), 2.02–1.95 (1H, m, piperidine H-4a), 1.66–1.46 (3H, m, piperidine H-5, 4b). ^{13}C NMR (125 MHz, $CDCl_3$) $\delta = 175.7$ (C=O, COOH), 162.5 (imine CH, C-3′), 152.7 (C, Ar–C, phenyl C-4), 149.5 (CH, Ar–C, phenyl C-5), 131.4 (CH, Ar–C, phenyl C-1), 124.6 (CH, Ar–C, phenyl C-2), 113.4 (CH, Ar–C, phenyl C-3), 112.8 (C, Ar–C, phenyl C-6), 60.7 (CH_2, C-1′), 57.8 (CH_2, C-2′), 56.7 (2 × CH_3, phenyl OCH_3), 55.7 (CH_2, piperidine C-2), 52.5 (CH_2, piperidine C-6), 40.7 (CH, piperidine C-3), 24.2 (CH_2, piperidine C-4), 22.1 (CH_2, piperidine C-5). Anal. calcd. for $C_{17}H_{24}N_2O_4$: C, 63.73; H, 7.55; N, 8.74. Found: C, 63.51; H, 7.53; N, 8.76.

1-(2-((3,4,5-trimethoxybenzylidene)amino)ethyl)piperidine-3-carboxylic acid (5u) Yield: 175 mg, 50.00%. FT-IR (KBr) ν_{max} 3219 (O–H), 3040 (Ar C–H), 2873 (C–H), 1711 (C=O), 1620 (C=N), 1581 (Ar C=C). ^{1}H NMR (500 MHz, $CDCl_3$) $\delta = 11.39$ (s, 1H, COOH), 8.24 (s, 1H, H-3′, imine CH=N), 6.87 (2H, s, phenyl H-2, 6, Ar–H), 3.83 (6H, s, 2 × OCH_3), 3.79 (2H, t, $J = 4.9$ Hz, H-2′, C=NCH_2), 3.68 (3H, s, OCH_3), 3.51 (1H, dd, $J = 12.5$, 7.9 Hz, piperidine H-2a), 2.84 (2H, t, $J = 4.9$ Hz, H-1′, NCH_2), 2.69–2.53 (2H, m, piperidine H-2b, 6a), 2.28 (1H, dd, $J = 12.3$, 7.7 Hz, piperidine H-6b), 2.25–2.09 (1H, m, piperidine H-3), 1.76–1.58 (1H, m, piperidine H-4a), 1.52–1.39 (3H, m, piperidine H-5, 4b). ^{13}C NMR (125 MHz, $CDCl_3$) $\delta =$ 177.4 (C=O, COOH), 161.6 (imine CH, C-3′), 154.3 (2 × C, Ar–C, phenyl C-5, 3), 140.6 (C, Ar–C, phenyl C-4), 135.7 (C, Ar–C, phenyl C-1), 108.9 (2 × C, Ar–C, phenyl C-6, 2), 59.8 (CH_2, C-1′), 56.4 (3 × CH_3, phenyl OCH_3), 57.4 (CH_2, C-2′), 56.7 (CH_2, piperidine C-2), 54.2 (CH_2, piperidine C-6), 40.8 (CH, piperidine C-3), 25.2 (CH_2, piperidine C-4), 21.1 (CH_2, piperidine C-5). Anal. calcd. for $C_{18}H_{26}N_2O_5$: C, 61.70; H, 7.48; N, 7.99. Found: C, 61.85; H, 7.46; N, 7.80.

1-(2-((4-methylbenzylidene)amino)ethyl)piperidine-3-carboxylic acid (5v) Yield: 123 mg, 44.89%. FT-IR (KBr) ν_{max} 3229 (O–H), 3049 (Ar C–H), 2872 (C–H), 1718 (C=O), 1622 (C=N), 1591 (Ar C=C). ^{1}H NMR (500 MHz, $CDCl_3$) $\delta = 11.47$ (s, 1H, COOH), 8.18 (s, 1H, H-3′, imine CH=N), 7.51 (2H, d, $J = 7.5$ Hz, Ar–H, phenyl H-2, 6), 7.19 (2H, d, $J = 7.5$ Hz, Ar–H, phenyl H-3, 5), 3.69 (2H, t, $J = 4.9$ Hz, H-2′, C=NCH_2), 2.99 (1H, dd, $J = 12.3$, 7.7 Hz, piperidine H-2a), 2.76 (2H, t, $J = 4.9$ Hz, H-1′, NCH_2), 2.70—2.52 (2H, m, piperidine H-2b, 6a), 2.42 (1H, dd, $J =$ 12.3, 7.7 Hz, piperidine H-6b), 2.36 (3H, s, CH_3), 2.22–2.17 (1H, m, piperidine H-3), 2.03–1.96 (1H, m, piperidine H-4a), 1.67–1.49 (3H, m, piperidine H-5, 4b). ^{13}C NMR (125 MHz, $CDCl_3$) $\delta = 174.4$ (C=O, COOH), 161.24 (imine CH, C-3′), 142.5 (C, Ar–C, phenyl C-4), 132.4 (CH, Ar–C, phenyl C-1), 129.5 (2 × CH, Ar–C, phenyl C-3, 5), 128.4 (2 × C, Ar–C, phenyl C-6, 2), 59.6 (CH_2, C-1′), 55.7 (CH_2, C-2′), 55.5 (CH_2, piperidine C-2), 53.78 (CH_2, piperidine C-6), 41.1 (CH, piperidine C-3), 24.9 (CH_2, piperidine C-4), 23.6 (CH_2, piperidine C-5), 20.8 (CH_3, phenyl CH_3). Anal.

calcd. for $C_{16}H_{22}N_2O_2$: C, 70.04; H, 8.08; N, 10.21. Found: 69.79; H, 8.10; N, 10.18.

1-(2-((naphthalen-2-ylmethylene)amino)ethyl)piperidine-3-carboxylic acid (5w) Yield: 149 mg, 48.06%. FT-IR (KBr) ν_{max} 3239 (O–H), 3039 (Ar C–H), 2881 (C–H), 1710 (C=O), 1618 (C=N), 1588 (Ar C=C). ^{1}H NMR (500 MHz, $CDCl_3$) $\delta = 11.6$ (s, 1H, COOH), 8.10 (s, 1H, H-3′, imine CH=N), 8.08–7.26 (7H, m, Ar–H, napthyl H), 3.89 (2H, t, $J = 4.8$ Hz, H-2′, C=NCH_2), 3.08 (1H, dd, $J = 12.3$, 7.7 Hz, piperidine H-2a), 2.81 (2H, m, H-1′, NCH_2), 2.74–2.57 (2H, m, piperidine H-2b, 6a), 2.47 (1H, dd, $J = 12.5$, 7.7 Hz, piperidine H-6b), 2.38–2.30 (1H, m, piperidine H-3), 2.25–2.12 (1H, m, piperidine H-4a), 1.87–1.60 (3H, m, piperidine H-5, 4b). ^{13}C NMR (125 MHz, $CDCl_3$) $\delta =$ 176.4 (C=O, COOH), 162.4 (imine CH, C-3′), 134.9 (C, Ar–C, phenyl C-4), 133.8 (C, Ar–C, phenyl C-9), 133.5 (CH, Ar–C, phenyl C-1), 129.7 (CH, Ar–C, phenyl C-8), 129.3 (CH, Ar–C, phenyl C-3), 129.0 (CH, Ar–C, phenyl C-10), 128.4 (CH, Ar–C, phenyl C-5), 126.98 (C, Ar–C, phenyl C-2), 126.92 (C, Ar–C, phenyl C-6), 126.4 (C, Ar–C, phenyl C-7), 59.5 (CH_2, C-1′), 55.4 (CH_2, C-2′), 55.3 (CH_2, piperidine C-2), 53.7 (CH_2, piperidine C-6), 40.9 (CH_2, piperidine C-3), 24.9 (CH_2, piperidine C-4), 22.6 (CH_2, piperidine C-5). Anal. calcd. for $C_{19}H_{22}N_2O_2$: C, 73.52; H, 7.14; N, 9.03. Found: C, 73.77; H, 7.13; N, 9.05.

1-(2-((4-(trifluoromethoxy)benzylidene)amino)ethyl)piperidine-3-carboxylic acid (5x) Yield: 187 mg, 54.36%. FT-IR (KBr) ν_{max} 3237 (O–H), 3046 (Ar C–H), 2881 (C–H), 1712 (C=O), 1619 (C=N), 1579 (Ar C=C), 1356 (C–F). ^{1}H NMR (500 MHz, $CDCl_3$) $\delta = 11.55$ (s, 1H, COOH), 8.27 (s, 1H, H-3′, imine CH=N), 7.55 (2H, d, $J = 7.5$ Hz, Ar–H, phenyl H-2, 6), 6.97 (2H, d, $J = 7.5$ Hz, Ar–H, phenyl H-3, 5), 3.60 (2H, t, $J = 5.3$ Hz, H-2′, C=NCH_2), 3.05 (1H, dd, $J = 12.3$, 7.7 Hz, piperidine H-2a), 2.89 (2H, t, $J = 5.3$ Hz, H-1′, NCH_2), 2.77–2.67 (2H, m, piperidine H-2b, 6a), 2.66 (1H, dd, $J = 12.5$, 7.7 Hz, piperidine H-6b), 2.28–2.20 (1H, m, piperidine H-3), 2.11–1.98 (1H, m, piperidine H-4a), 1.79–1.57 (3H, m, piperidine H-5, 4b). ^{13}C NMR (125 MHz, $CDCl_3$) $\delta = 173.4$ (C=O, COOH), 161.8 (imine CH, C-3′), 152.6 (C, Ar–C, phenyl C-4), 134.8 (CH, Ar–C, phenyl C-1), 129.4 (2 × CH, Ar–C, phenyl C-6, 2), 121.8 (q, $J_{C,F} = 325.1$, 193.1 Hz, C, OCF_3), 121.2 (2 × C, Ar–C, phenyl C-5, 3), 60.1 (CH_2, C-1′), 57.5 (CH_2, C-2′), 56.4 (CH_3, phenyl OCH_3), 55.8 (CH_2, piperidine C-2), 52.6 (CH_2, piperidine C-6), 40.4 (CH, piperidine C-3), 23.4 (CH_2, piperidine C-4), 21.5 (CH_2, piperidine C-5). Anal. calcd. for $C_{16}H_{19}F_3N_2O_3$: C, 55.81; H, 5.56; N, 8.14. Found: C, 55.63; H, 5.57; N, 8.11.

1-(2-((3-(trifluoromethyl)benzylidene)amino)ethyl)piperidine-3-carboxylic acid (5y) Yield: 176 mg, 53.66%. FT-IR (KBr) ν_{max} 3243 (O–H), 3068 (Ar C–H), 2878 (C–H), 1719 (C=O), 1616 (C=N), 1588 (Ar C=C), 1346 (C-F). ^{1}H NMR (500 MHz, $CDCl_3$) $\delta = 11.33$ (s, 1H, COOH), 8.46 (s, 1H, H-3′, imine CH=N), 7.89–7.25 (m, 4H, phenyl H-2,4,5,6, Ar–H), 3.77 (2H, t, $J = 5.1$ Hz, H-2′, C=NCH_2), 3.06 (1H, dd, $J = 12.5$, 7.7 Hz, piperidine H-2a), 2.87 (1H, t, $J = 5.0$ Hz, H-1a′, NCH_2), 2.81–2.65 (3H, m, H-1b′, NCH_2, piperidine H-2b, 6a), 2.53–2.29 (2H, m, piperidine H-3, 6b), 2.23–2.07 (1H, m, piperidine H-4a), 1.88–1.64 (3H, m, piperidine H-5, 4b). ^{13}C NMR (125 MHz, $CDCl_3$) $\delta = 176.4$ (C=O, COOH), 162.1(imine CH, C-3′), 137.0 (CH, Ar–C, phenyl C-1), 129.75 (C, Ar–C, phenyl C-2), 129.73 (CH, Ar–C, phenyl C-5), 129.6 (CH, Ar–C, phenyl C-4), 129.0 (q, $J_{C,F} = 33.2$ Hz, CH, Ar–C, phenyl C-3), 124.1 (CH, Ar–C, phenyl C-6), 123.6 (q, $J_{C,F} = 272.5$ Hz, CF_3), 59.5 (CH_2, C-1′), 55.4 (CH_2, C-2′), 55.3 (CH_2, piperidine C-2), 53.7 (CH_2, piperidine C-6), 40.9 (CH, piperidine C-3), 24.9 (CH_2, piperidine C-4), 22.6 (CH_2, piperidine C-5). Anal. calcd. for $C_{16}H_{19}F_3N_2O_2$: C, 58.53; H, 5.83; N, 8.53. Found: C, 58.69; H, 5.81; N, 8.51.

Determination of partition coefficient (log *P*)

Log *P* value of all the synthesized compounds (**5a**–**5y**) was determined experimentally by shake flask method in *n*-octanol and buffer (pH 7.4) as per the reported procedure (Ghadimi et al. 2008). A calibration curve was plotted using different concentrations of the compound in water using methanol as co-solvent. The known quantity compounds were dissolved separately in *n*-octanol and shaken with the buffer on a mechanical shaker for 30 min. To accomplish complete phase separation, the mixture was centrifuged for 20 min, and the *n*-octanol phase was separated. The absorbance of the buffer phase was then measured, and the Log *P* was calculated by correlating the absorbance with the concentration in the standard plot.

Pharmacology

In vitro PAMPA-BBB assay

PAMPA-BBB assay was performed to predict the in vivo penetration of the synthesized compounds (**5a**–**5y**) across BBB by the reported method (Di et al. 2003). The porcine polar brain lipid (PBL) was obtained from the Avanti Polar Lipids. Dodecane was purchased from the Avra Synthesis Pvt. Ltd. Acceptor microplates with PVDF membrane pore size 0.45 µm and donor microplates were procured from the Merck Millipore. The test compounds were dissolved in dimethylsulfoxide (DMSO) to form the primary stock solutions (5 mg/mL). An aliquot of 10 µL from each primary stock solution was diluted 200 times using a buffer of pH 7.5 to form the corresponding secondary stock solutions

(25 µg/mL). The donor wells were filled with 200 µL of the secondary stock solution. The coating of the porous filter disk at the bottom of each well of the acceptor plate was accomplished using a solution of PBL in an inert organic solvent (4 µL of 20 mg/mL PBL in dodecane). 200 µL of buffer (pH 7.4) was then filled into the acceptor plate. The acceptor plate was then carefully stacked over the donor plate to create the sandwich and incubated for 18 h to allow the diffusion of the test compound from the donor well to the acceptor well via lipid membrane. The drug concentration in the acceptor, donor, and reference well was then determined by UV spectroscopy (96 well UV microplate reader). The samples were scanned in triplicate for at least five different wavelengths. The validation of the model was done by using nine commercial drugs with known BBB permeability which were purchased from Sigma-Aldrich (India). A linear correlation was established by using the experimentally obtained permeability [$P_{e\ (Exp)}$] and reference permeability [$P_{e\ (Ref)}$] (Di et al. 2003).

Animals

In vivo experiments were performed on Swiss albino mice (20 ± 5 g) of either sex, which were procured from the Central Animal House, Institute of Medical Sciences, Banaras Hindu University, Varanasi. The animals were housed in polypropylene cages at a controlled temperature of 25 ± 1 °C and 45–55% relative humidity, under 12:12 h light/dark cycle. The rodents had free access to commercial food pellets and water ad libitum unless stated otherwise. Rodents were allowed to acclimatize with the laboratory environment before experiments for at least 1 week. Periodical measurement of the body weight of animals was done, and the animals were given identification marks cryptically encoding the group as well as dose level. Principles of laboratory animal care guidelines (NIH publication number 85–23, revised 1985) were followed. All the experimental procedures and protocols have been approved by the Institutional Animal Ethical Committee, Institute of Medical Sciences, Banaras Hindu University, Varanasi (Letter No. Dean/12–13/CAEC/17).

sc-PTZ induced seizures in mice

The mice model of *sc*-PTZ induced seizures as described by Kowalczyk et al. 2014; was used to screen the compounds **5d, 5f, 5j, 5l, 5m, 5n, 5w, 5x** and **5y**. These compounds exhibited better permeability in PAMPA-BBB assay (Kowalczyk et al. 2014). Clonus of the whole body lasting more than 3 s followed by loss of righting reflex is an indicator of seizures in this test. Delay in the onset of seizures and reduced frequency by test and the standard drug is considered as anti-epileptic activity. The PTZ was procured from Sigma Aldrich and administered *s.c.* at the dose of 100 mg/kg. Test compounds and a standard drug (tiagabine) were administered i.p. 1 h before PTZ challenge at equimolar dose relative to 10 mg/kg tiagabine. Control group animals received physiological saline (0.9%) containing 2.5% tween 80. Latency to first seizure and frequency of seizures were noted up after PTZ administration.

DMCM induced seizures in mice

Compounds eliciting considerable anticonvulsant activity in the *sc*-PTZ model were further screened using the standard DMCM induced seizure model (Andersen et al. 2001a). This test measures the efficiency of drugs to delay the onset of tonic and clonic seizures caused by DMCM. Test compounds (**5d, 5l, 5w, 5x** and **5y**) were injected i.p. at the dose of 10 mg/kg equivalent to standard tiagabine. DMCM was injected at the dose of 15 mg/kg, i.p. The latency to the first convulsion was noted.

Rota-rod performance test in mice

The test is used to observe any motor incoordination caused by the drugs. The test involves measurement of fall off time of mice on a rotating rod (10 rpm). The test was conducted in two sessions- before drug treatment and 1 h after drug treatment. Only those animals that stay more than 3 min on rotating rods were selected for the test. Each mouse was placed on rotating rod and "fall-off" time was noted. Immediately after the test animals were treated with the respective drug, i.e., test, standard, and the vehicle in case of control. One hour after the drug treatment, animals were again placed on rotating rod and "fall-off" time was noted.

MTT assay for the measurement of cell viability

The effect of the most active compounds (**5d, 5w**, and **5y**) on neuroblastoma cell line SH-SY5Y (procured from National Center for Cell Science, Pune) was evaluated by MTT assay (Regulska et al. 2010; Shidore et al. 2016). Initially, 96-well plates were seeded with SH-SY5Y cells at a density of 1×10^5/well in 100 µL of the medium, followed by 24 h of incubation at 37 °C in 5% CO_2. Different concentrations of the test compounds (ranging from 1 µM to 160 µM) were then incubated with the cells for further 24 h. After the exposure of cells to the different concentrations of the test drugs, 20 µL of 5 mg/mL MTT reagent was added to each well and incubated for 3 h (at 37 °C, 5% CO_2). After incubation, the formation of a purple colored precipitate was observed under a microscope and solubilized by adding 1 mL of DMSO. Cell viability was measured by determining absorbance at 570 nm in a microplate-reader (Synergy HTX, BioTek, Germany). The outcomes were expressed as

a growth percentage in each well relative to the control cells incubated in the absence of test compounds. Percentage cell viability was measured by using the following formula:

$$Percentage\ Cell\ Viability = Absorption\ of\ sample / absorption\ of\ control \times 100$$

Statistical analysis

The experimental results are expressed as the mean ± S.D ($n = 6$) followed by a one-way analysis of variance. Tukey's multiple comparisons test were applied for determining the statistical significance between different groups. InStat Graph Pad Software (San Diego, CA, USA) was used for all statistical analyses and a p-value <0.05 was considered significant.

Computational studies

Homology modeling of GAT1

Homology modeling was performed as per the method of Zaman and coworkers (Singh et al. 2017). It was carried out in three principle steps. The first step involves the alignment of the amino acid sequence of Drosophila dopamine transporter (dDAT) with that of the target sequence (GAT-1). The second step includes model building from the alignment, followed by validation.

From UniProt website (http://www.uniprot.org/uniprot/P30531) the complete sequence of human sodium-dependent and chloride-dependent GABA transporter 1 (GAT1) (UniProtKB: P30531) was downloaded. To find the suitable template psi-BLAST was performed against Protein Data Bank (PDB). A template of *Drosophila melanogaster* dopamine transporter (dDAT) (PDB ID: 4XP4_A) (Wang et al. 2015) was chosen as the template for building multiple homology models. The sequences of the template (4XP4_A) GAT1 were aligned using multiple sequence alignment programs (Clustal W). The generated models were then subjected to loop refinement using the Prime module implemented in the Schrödinger suite. During model preparation, the Na^+ and Cl^- ions were retained. The quality of the models was assessed by using Ramachandran plot. The best model was validated by docking tiagabine (a known inhibitor) which matches with the previous studies and mutagenesis data.

In silico docking simulations

In silico docking simulation protocols were performed using Schrödinger Glide module in Schrödinger Suite 10.5.014 MM Share Version 3.3.014 Release 2016-1 with workstation 4× Intel(R) Xeon(R) CPU E5-1607 v3 @ 3.10 GHz on Kernel Linux operating environment. The potential ligands **5d**, **5w**, and **5y** were selected and prepared using LigPrep module. The minimum energy conformers of selected ligands were generated using OPLS2005 force field. Homology modeled protein structure (PDB Code: 4XP4) of GAT1 GABA transporter (GAT) was refined and corrected using Protein Preparation Wizard module. The structure of the protein was further optimized using PropKa method at default pH value 7.0, and restrained minimization was performed for heavy atoms to RMSD 0.30 Å. Receptor Grid was generated surrounding the active binding pocket of the protein. The grid box of 10 Å was created by supplying the x, y and z coordinates ($x = 29$ Å, $y = 27$ Å and $z = 22$ Å) surrounding the active pocket in which the tiagabine binds. The prepared grid and docking simulation protocols of Glide (Grid-Based Ligand Docking with Energetics) extra precision (XP) mode were validated by docking the tiagabine. During the docking simulations, the protein was kept rigid, and ligands were kept flexible. All other parameters of Glide module were maintained at their default values. The docking results were studied using the Glide XP visualizer module to gain insights of the interactions of ligands with the amino acid residues. The results of score and interactions were analyzed in comparison to tiagabine.

Molecular dynamics simulations

To confirm the stability of binding mode interactions for the most potent compound **5w**, its docked complex was further utilized for molecular dynamics simulation run using the Desmond module of Schrödinger Maestro 10.5.014 program with an OPLS-AA force field in an explicit solvent with the TIP3P water model. The docked complex of **5w** with GABA GAT1 transporter protein (PDB Code: 4XP4) was soaked adequately in 14,594 TIP3P water molecules, and the system was neutralized by adding $4Na^+$ ions to balance the overall charge of the system. The generated system with water molecules consisted of total 52,414 atoms. The system was further minimized to maximum 20,000 steps. The recording interval energy was kept at 1.2 ps, and the trajectory was set at 9.6. At constant number of atoms (N), pressure (P), and temperature (T) (NVT) molecular dynamics was performed for the first 100 ps, during which the temperature of the system was raised from 0–300 K. For further simulations, the system was maintained at constant temperature (300 K) and pressure (1.0132 bar) till the complete cycle of 50 ns simulation run.

In silico ADME studies

QikProp module of Schrödinger Maestro 10.5.014 Release 2016-1 was used to predict the "drug likeliness" of the most

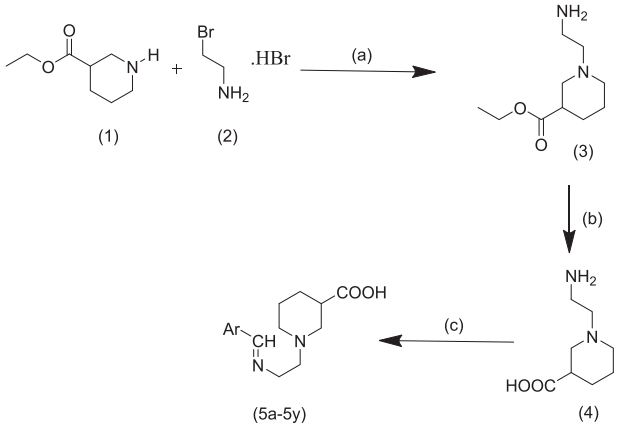

Scheme 1 Synthesis of compounds **5a**–**5y**; Reagents and conditions: **a** K_2CO_3, KI, 1,4-dioxane, reflux, 30 h; **b** (i) 3 N NaOH, EtOH, RT, (ii) 1 N HCl; **c** Corresponding aromatic aldehydes, glacial acetic acid (2–3 drops), EtOH, reflux, 3–6 h

active compounds **5d**, **5w**, and **5y**. Before being subjected to QikProp analysis, the best-fit ligands were neutralized. Several principal descriptors were estimated.

Results and discussion

Chemistry

The synthesis of the target compounds **5a**–**5y** was performed according to the reaction sequence outlined in Scheme 1. At the outset, Ethyl 1-(2-aminoethyl)piperidine-3-carboxylate (**3**) was synthesized by piperidine-3-carboxylic acid ethyl ester (**1**) and 2-bromoethylamine hydrobromide (**2**) by nucleophilic substitution (SN^2) reaction. Compound **3** which is an ester derivative of the parent cyclic amine (nipecotic acid) was used for protecting carboxyl group in the reaction. The ethyl ester group of compound **3** was hydrolyzed in alcoholic alkaline solution to generate compound **4**. Compounds **5a**–**5y** were synthesized by the nucleophilic addition of the amino group of compound **4** to the carbonyl group of corresponding aromatic aldehydes forming an unstable aminomethanol intermediate followed by dehydration in an acidic environment to generate an imine (Scheme 1).

The structures of the synthesized compounds were ascertained by FT-IR, ^{1}H NMR, ^{13}C NMR and elemental analysis. The amino group in compound **3** was confirmed by the presence of asymmetric N–H stretching around 3366 cm^{-1} and symmetric N–H stretching around 3298 cm^{-1}, respectively. The characteristic broad O–H stretching peak observed at around 3236 cm^{-1} in compound **4** depicted the presence of H-bonded O–H group. The absorption bands in the compounds **5a**–**5y** showed characteristic skeletal frequencies for C=O and C=N at 1729–1706 and 1628–1612 cm^{-1}, respectively. A singlet varying from δ_H11.6–11.18 ppm in ^{1}H NMR belonged to piperidine-CO–O**H**, and the singlet appeared at δ_H9.02–8.10 ppm revealed the presence of N = C**H**– methaneimine protons. The chemical shifts from 181.2–172.9 and 164.3–156.7 ppm in ^{13}C NMR confirmed the existence of **C**=O and **C**=N, respectively. Results of the elemental analysis were found within ± 0.4% of the theoretical values and were well within the limit. The

Table 1 Chemical structures and physicochemical properties of the synthesized compounds (**5a**–**5y**)

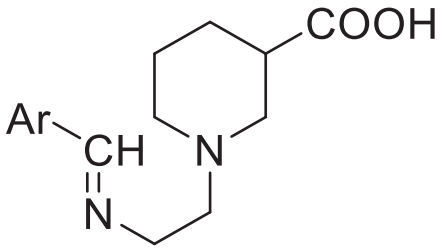

Comp.	Ar–group	R_f[a]	Log P[b]	Melting point (°C)
5a	Phenyl	0.46	2.36	192–194
5b	2-Chlorophenyl	0.37	2.62	162–164
5c	4-Chlorophenyl	0.37	2.60	167–169
5d	2,3-Dichlorophenyl	0.30	3.16	181–183
5e	2,4-Dichlorophenyl	0.28	3.31	172–174
5f	2,3,6-Trichlorophenyl	0.26	3.48	187–189
5g	3-Fluorophenyl	0.43	2.42	158–160
5h	4-Fluorophenyl	0.42	2.46	166–168
5i	2,4-Difluorophenyl	0.41	2.51	177–179
5j	3,4,5-Trifluorophenyl	0.34	2.90	186–188
5k	3-Bromophenyl	0.29	3.28	155–157
5l	4-Bromophenyl	0.31	3.20	158–160
5m	2,6-Dibromophenyl	0.27	3.47	148–150
5n	4-Nitrophenyl	0.25	3.41	212–214
5o	2-Nitrophenyl	0.26	3.37	222–224
5p	2-Hydroxyphenyl	0.52	2.12	198–200
5q	4-Hydroxyphenyl	0.56	2.08	213–215
5r	3-Methoxyphenyl	0.49	2.27	204–206
5s	4-Methoxyphenyl	0.48	2.29	209–211
5t	3,4-Dimethoxyphenyl	0.51	2.18	224–226
5u	3,4,5-Trimethoxyphenyl	0.54	2.10	217–219
5v	4-Methylphenyl	0.35	2.82	177–179
5w	Napthyl	0.28	3.42	228–230
5x	4-Trifluoromethoxyphenyl	0.24	3.78	163–165
5y	3-Trifluoromethylphenyl	0.30	3.27	181–183

[a]R_f values are determined using DCM/methanol (9.5:0.5) as mobile phase

[b]Log P values of all the compounds were determined experimentally using shake flask method

partition co–efficient was determined using the octanol/water "shake-flask" method. The R_f values, melting point and Log P values of the compounds **5a**–**5y** are presented in Table 1.

Pharmacology

PAMPA-BBB assay

Determination of brain permeability is very crucial for antiepileptic drugs to reach the target site and elicit its effect. PAMPA-BBB is a technique to observe the BBB permeation of drug molecules. In the current work, the permeability of the synthesized compounds was evaluated by PAMPA-BBB as per the reported procedure of Di et al. (Di et al. 2003) This system is a prototype of BBB that measures the effective permeability (P_e, cm/s) of an artificial lipid membrane and thereby predicts the rate of transcellular passive diffusion of drugs across the BBB. A plot of experimentally obtained permeability [$P_{e(Exp)}$] versus permeability reported in the literature [$P_{e(Ref)}$] provided a good linear correlation $P_{e(Exp)} = 1.308\ P_{e(Ref)} - 0.8394$ ($R^2 = 0.9317$). Using this equation, we have calculated the cut-off limits for determining the BBB permeability of the test compounds. The values of $P_{e(Ref)}$ were taken from the limits established by Di et al. The findings suggested that the compounds **5d**, **5f**, **5j**, **5l**, **5m**, **5n**, **5w**, **5x**, and **5y** exhibited considerable permeability across BBB. **5w** was more permeable ($P_e = 8.93$) than the standard tiagabine ($P_e = 7.96$) (See Supplementary Table S1)

PTZ-induced convulsions in mice

Manipulation of GABA metabolism, synaptic uptake mechanism and its receptor complex along with neuronal ion channels has been a central theme for research to discover safe and effective novel drugs for the treatment of epilepsy. Tiagabine is a recent entrant in the category of anti-epileptic drug that has a distinct mechanism of reuptake inhibition of GABA at the synapse. Tiagabine augments the level and neuro-inhibitory activity of GABA by interfering the function of GATs specifically GAT1.

Subcutaneous injection of PTZ is validated and most commonly used rodent model of epilepsy. In this test inhibitory potential of test drugs to suppress or delay the seizures induced by PTZ is measured. It was observed that the test compounds **5d**, **5l**, **5w**, **5x** and **5y** significantly delayed the onset of seizures and its frequency. However, compounds **5n**, **5f**, **5m**, **and 5j** failed to exhibit anti- seizure activity in this model (Table 2). Tiagabine also significantly delayed the onset of seizures and frequency of seizures. **5d**, **5w**, and **5y** were most potent amongst synthesized compounds.

Table 2 Effect of drugs on s.c. administered PTZ-induced seizures

Comp.	Latency of seizures (s)[a]	Frequency of seizures (numbers)[a]
Control	554.16 ± 18.84	4.33 ± 0.81
5d	1036.50 ± 20.56*	1.66 ± 0.81*
5f	555.33 ± 12.82	3.66 ± 0.81
5j	564.16 ± 25.46	3.83 ± 0.75
5l	843.16 ± 21.94*	1.83 ± 0.75*
5m	560.83 ± 19.45	4.33 ± 0.81
5n	565.16 ± 46.82	4.16 ± 0.75
5w	1181.66 ± 19.16*	1.16 ± 0.40*
5x	792.33 ± 19.59*	2.16 ± 0.75*
5y	1119.83 ± 21.84*	1.33 ± 0.51*
Tiagabine	1276.33 ± 17.50*	1.16 ± 0.40*

Control: Physiological saline (0.9%) containing 2.5% tween 80; Tiagabine: 10 mg/kg, i.p.; all the test compounds were administered intraperitoneally at an equimolar dose relative to 10 mg/kg tiagabine

*$p < 0.05$ compared to control

[a]Values are expressed as the Mean ± SD ($n = 6$)

Table 3 Effect of compounds on DMCM induced seizures

Comp.	Latency of seizures (s)[a]
Control	222.33 ± 6.02
5d	373.33 ± 8.35*
5l	272.33 ± 11.62*
5w	417.83 ± 9.17*
5x	267.66 ± 13.93*
5y	411.50 ± 16.67*
Tiagabine	438.66 ± 10.46*

Control: Physiological saline (0.9%) containing 2.5% tween 80; Tiagabine: 10 mg/kg, i.p.; all the test compounds were administered intraperitoneally at an equimolar dose relative to 10 mg/kg Tiagabine

[a]Values are expressed as the Mean ± SD ($n = 6$)

*$p < 0.05$ compared to control

DMCM (Methyl-6,7-dimethoxy-4-ethyl-β-carboline-3-carboxylate)-induced seizures in mice

Only those compounds that exhibited significant anti-epileptic activity in the sc-PTZ model were selected for further screening in DMCM induced seizure test. DMCM is a potent convulsant agent having dual effect-augmenting excitatory amino acid and attenuating GABA inhibitory function. DMCM has been identified to possess specific benzodiazepine binding sites (Petersen 1983). The outcome of the model was similar to that of sc-PTZ induced seizure model. All the test compounds (**5d**, **5l**, **5w**, **5x** and **5y**) and standard drug significantly delayed the onset of convulsion (Table 3).

Rota-rod performance test in mice

Drugs acting on CNS do have potential to cause motor incoordination. In order to assess the putative motor incoordination effect of drugs, rota rod test is widely used. In this test rodents are placed on a rotating rod and fall off time is measured before and after the drug treatment. A significant decrease in the fall off time indicates the motor incoordination effect of the drug. In this test, all the test compounds were found to be devoid of any adverse effect on muscle coordination (Table 4). Standard drug diazepam showed a significant reduction in fall off time.

Cell viability and neurotoxicity

Some antiepileptic drugs and their metabolites have been reported to possess neurotoxicity (Araújo et al. 2004; Ambrósio et al. 2000; Liu et al. 2015; Gao and Chuang 1992; Gao et al. 1995; Nonaka et al. 1998). Ideally, antiepileptic drugs should prevent the seizures without producing neuronal toxicity. Therefore, the therapeutic suitability of the most active compounds (**5d, 5w**, and **5y**) and their effects on cell viability was determined in neuroblastoma cell line (SH-SY5Y). The ability of intracellular dehydrogenases to reduce MTT to form the insoluble formazan is interpreted as the measure of cell viability. The formazan upon solubilization can be measured spectrophotometrically, which is directly proportional to the viable cell number (Lim et al. 2015). The results of the experiment reveal that the MTT reduction was not effected significantly by test compounds (**5d, 5w**, and **5y**), thus corresponds to the insignificant cell death in the concentrations of the test compounds ranging from 1 µM to 80 µM (Table 5).

Table 4 Effect of compounds on rota-rod performance test in mice

Comp.	Fall off time before treatment (s)[a]	Fall off time after treatment (s)[a]
Control	318.33 ± 11.37	326.66 ± 12.95
5d	323.50 ± 6.41	328.16 ± 5.56
5w	331.83 ± 15.06	333.33 ± 8.23
5y	325.16 ± 16.64	331.83 ± 15.35
Tiagabine	320.83 ± 13.07	322.66 ± 5.98
Diazepam	334.83 ± 15.86	152.66 ± 12.12[a]

Control: Physiological saline (0.9%) containing 2.5% tween 80; Tiagabine: 10 mg/kg, i.p.; Diazepam: 4 mg/kg, i.p.

All the test compounds were administered intraperitoneally at an equimolar dose relative to 10mg/kg tiagabine

*$p < 0.05$ compared to control

[a]Values are expressed as the Mean ± SD ($n = 6$)

Computational studies

Homology modeling

For model building, human GAT1 protein has been selected. Structures are accessible for dDAT, which is one of the closest transporter protein related to human GAT1. Homology model of both the occluded and the open-to-out conformations was constructed taking dDAT structure as a template (See Supplementary Fig. S7). After the alignment, 46% sequence identity and 67% similarity of the 4XP4 template with GAT1 sequence has been obtained. In the model generation, a known disulfide bridge between C164 and C173 located in the extracellulAr–loop 2 of GAT1 was included (Jurik et al. 2015). A total of 10 models were prepared using the knowledge-based method implemented in the Schrödinger Suite 2016 (Kim and Cho 2016). The best model thus generated was then subjected to loop refinement. In the Ramachandran plot, all the amino acids except Phe174 and Ser178 were present in the favored/allowed regions, which enabled to use the best model for the docking study (See Supplementary Fig. S8). These two residues are not the part of the binding site. The models were exhaustively tested and verified through comparison to functional and mutational data reported in the literature. The homology model was evaluated through computations of molecular interactions fields and sequence identities. Template in an open-to-out conformation was used for allowing access to bulky synthesized molecules. A validated homology model was finally obtained followed by the identification of putative spots for ligand (Tiagabine)

Table 5 Cell Viability of the test compounds at different concentrations in neuroblastoma cell line (SH-SY5Y)

Comp.	Percentage cell viability[a]				
	1 µm	10 µm	20 µm	40 µm	80 µm
5d	99.99 ± 0.054	99.95 ± 0.101	99.91 ± 0.115	98.63 ± 0.059	89.25 ± 0.116
5w	99.74 ± 0.127	99.46 ± 0.220	96.50 ± 0.380	92.22 ± 0.467	83.52 ± 0.304
5y	99.60 ± 0.117	99.40 ± 0.216	95.81 ± 0.378	91.48 ± 0.470	84.92 ± 0.384

Values are expressed as the percentage cell viability ± SD of at least five independent experiments

[a]Percentage cell viability of SH-SY5Y cells incubated with increasing concentration of test compounds

selectivity. Tiagabine was added as a co-crystallized ligand in the model which was further utilized for molecular docking and dynamics.

In silico docking study

In silico docking studies were performed using the Schrödinger Maestro program to gain insight into the possible mode of protein–ligand interactions using a generated and validated model of GAT1 GABA transporter (PDB Code: 4XP4). The validation of the prepared grid and docking protocols was performed by generating a minimum energy conformer of tiagabine, and it's docking on a prepared grid. The results demonstrate that tiagabine occupied the same active site within the binding pocket leading to its complementary interaction with the amino acid residues within the active site (Petrera et al. 2016; Skovstrup et al. 2010; Jurik et al. 2013) (Fig. 2).

The binding affinity of the active compounds **5d, 5w** and **5y** were carried out using GAT1 GABA transporter modeled protein. The molecular docking studies yielded the best possible conformation for all the ligands **5d** (Glide Score: −3.9); **5w** (GLIDE Score: −6.2) and **5y** (GLIDE Score: −7.3) occupying the similar binding pocket as that of tiagabine (GLIDE Score: −4.6) (See Supplementary Fig. S9, S10 and S11). In the present study, the active binding pocket was selected on the basis of the outcomes of Petrera et al. The active pocket was present around the amino acid residues Tyr60, Ala61, Gly63, Gly65, Trp68, Arg69, Tyr139, Tyr140, Ile143, Gln291, Phe294, Ser295 and Na atom.

The docking conformations of the compounds **5d, 5w**, and **5y** reveal salt bridge formation between oxygen (O) atom of carboxyl group and sodium (Na611). Another oxygen (O) atom present in carboxyl group of compound **5y** shown to have additional metal coordination interaction with sodium (Na611). The O atom of the carboxyl group in all the docked ligands interacted through a network of hydrogen bonding with backbone atom of Gly65. Compounds **5d** and **5w** involved in the hydrogen bonding with side chain hydroxyl groups of Tyr140. Additionally, the NH group of all the ligands was also involved in hydrogen bonding interactions with Phe294 similar to tiagabine. The NH group of compound **5y** was additionally involved in π–cationic interaction with Tyr60. The charged interactions with Arg69 and Asp451 were also responsible for stabilizing the aromatic rings of the ligands. The detailed interaction results of tiagabine, **5d, 5w**, and **5y** with active site amino acid residues are summarized in Table 6. Overall, these interactions of all the docked ligands with the modeled protein of GAT1 GABA transporter showed complementary binding with active site amino acids residues as shown in Figs. 3, 4 and 5.

Molecular dynamics simulations

The dynamics simulation runs of the generated minimized complex of **5w** with GABA GAT1 transporter protein of

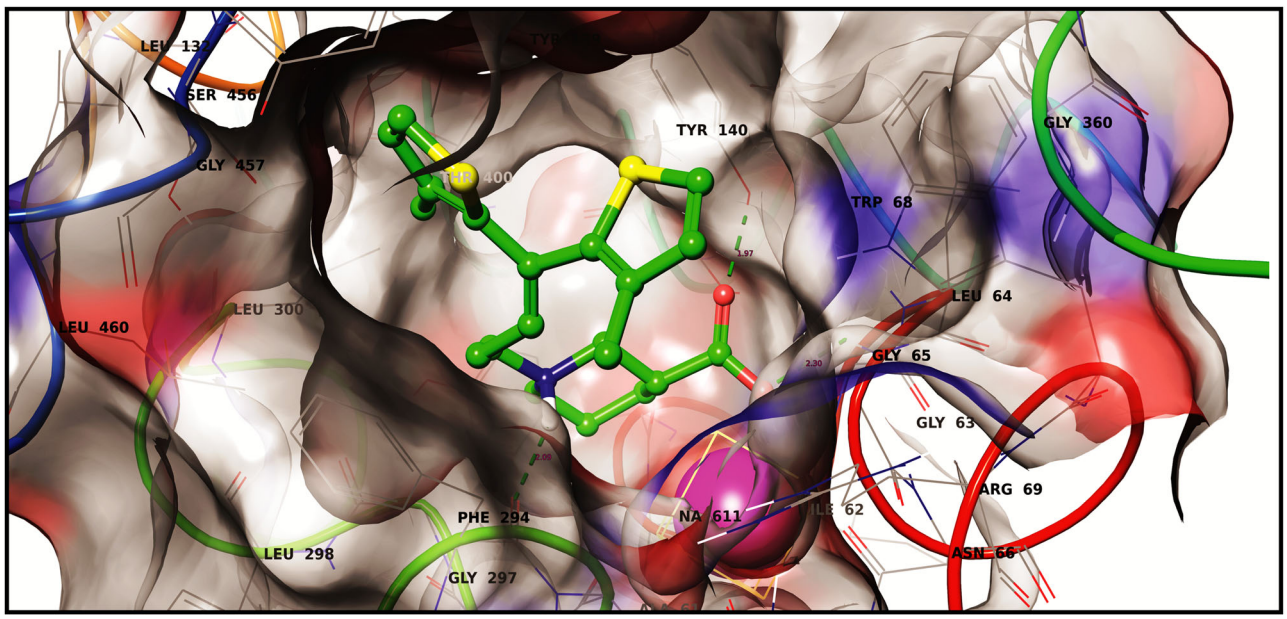

Fig. 2 3D Ribbon structure representation of docking conformation of the tiagabine in the hydrophobic pocket of modeled protein structure of GAT1 GABA transporter (PDB Code: 4XP4). Structure of tiagabine is shown as ball and stick model; light brown color surface is showing hydrophobic pocket; blue and red surface is charged surface of the protein; green dotted line is showing H-bonding interactions between active site amino acid residues and ligand

Table 6 Details of protein–ligand interactions of tiagabine, **5d, 5w**, and **5y**

Comp.	Parameters							
	Glide score	Interacting residues[a]						
		H-bonding	Salt bridge	Metal coordination	π–π cation	Hydrophobic	Polar	Charged
Tiagabine	−4.6	Gly65, Tyr140, Phe294	Na611	None	None	Tyr60, Ala61, Gly63, Trp68, Tyr139, Ile143, Gly297, Phe447	Asn66, Gln291, Ser295, Ser396	Arg69, Asp451
5d	−3.9	Gly65, Tyr140, Phe294	Na611	None	None	Tyr60, Ala61, Ile62, Gly63, Leu64, Trp68, Leu136, Tyr139, Gly297, Leu300, Leu460	Asn66, Ser295, Ser396	Arg69, Asp451
5w	−6.2	Gly65, Tyr140, Phe294	Na611	None	None	Tyr60, Ala61, Gly63, Leu64, Leu136, Tyr139, Tyr296, Gly297, Leu300, Ala455, Leu460	Asn66, Ser295, Ser396, Ser456	Asp451
5y	−7.3	Gly65, Phe294	Na611	Na611	Tyr60	Ala61, ile62, Gly63, Leu64, Leu136, Tyr139, Tyr140, Tyr296, Gly297, Leu300, Ala455, Leu460	Asn66, Ser396, Ser456	Asp451

[a]All the interactions of protein–ligand were observed within the distance of 4 Å

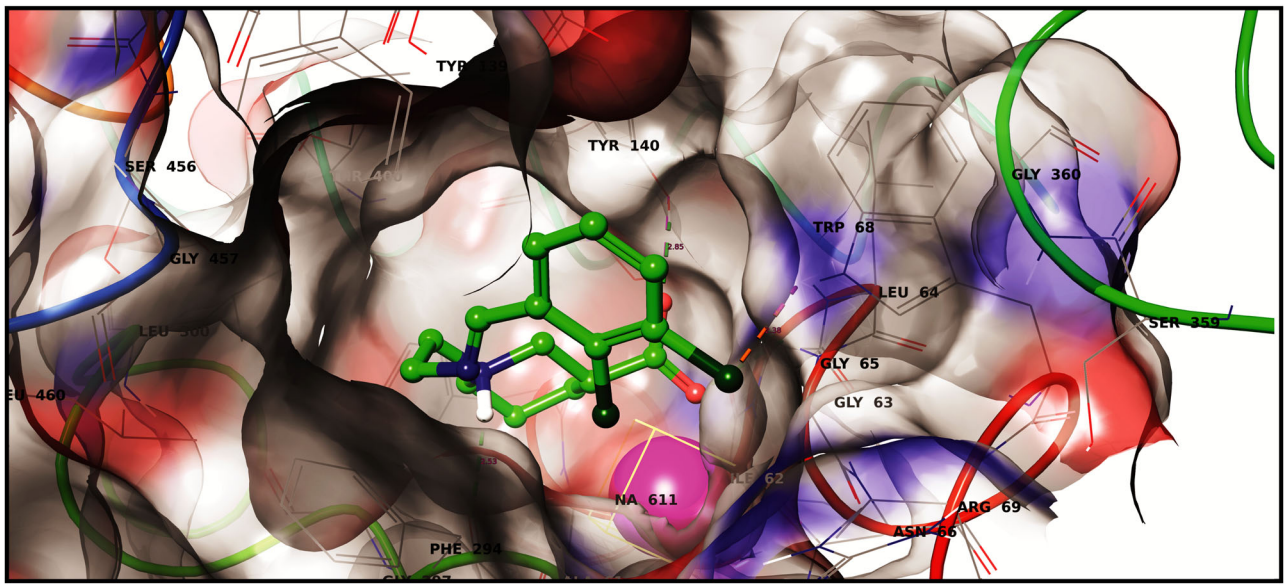

Fig. 3 3D Ribbon structure representation of docking conformation of the compound **5d** in the hydrophobic pocket of modeled protein structure of GAT1 GABA transporter (PDB Code: 4XP4). Structure of compound **5d** is shown as ball and stick model; light brown color surface showing hydrophobic pocket; the blue and red surface is charged surface of the protein; green dotted lines are H-bonding, and the red dotted line is charged interaction between active site amino acid residues and ligand

4XP4 was performed for 50 ns to predict the stability of binding mode interactions. The overall stability of the system was evaluated by RMSD (root mean square deviation) and RMSF (root mean square fluctuation) calculations. The results of the RMSD values confirmed that all frames of the complex were in trajectory throughout the simulation with average fluctuation in the range of 1–3 Å (See Supplementary, Fig. S12).

The graphical representation of binding interactions of compound **5w** showed the active site interactions throughout the simulation run (Fig. 6). The results demonstrated that compound **5w** efficiently interacted with active site residues Ala61, Gly65, Asn66, Arg69, Tyr140 and Phe294 through H-bonds. Besides, it also interacted with Phe294 through hydrophobic π-stacking. The carboxylate O atom also involved in salt bridge formation with Na611 atom.

The interaction fraction with individual amino acid residues was also calculated and represented in a stacked bar chart (Fig. 7). The interaction fraction of a percentage of total contact maintained throughout the run. For example, 0.8 suggests that interaction was maintained 80% of the total simulation run.

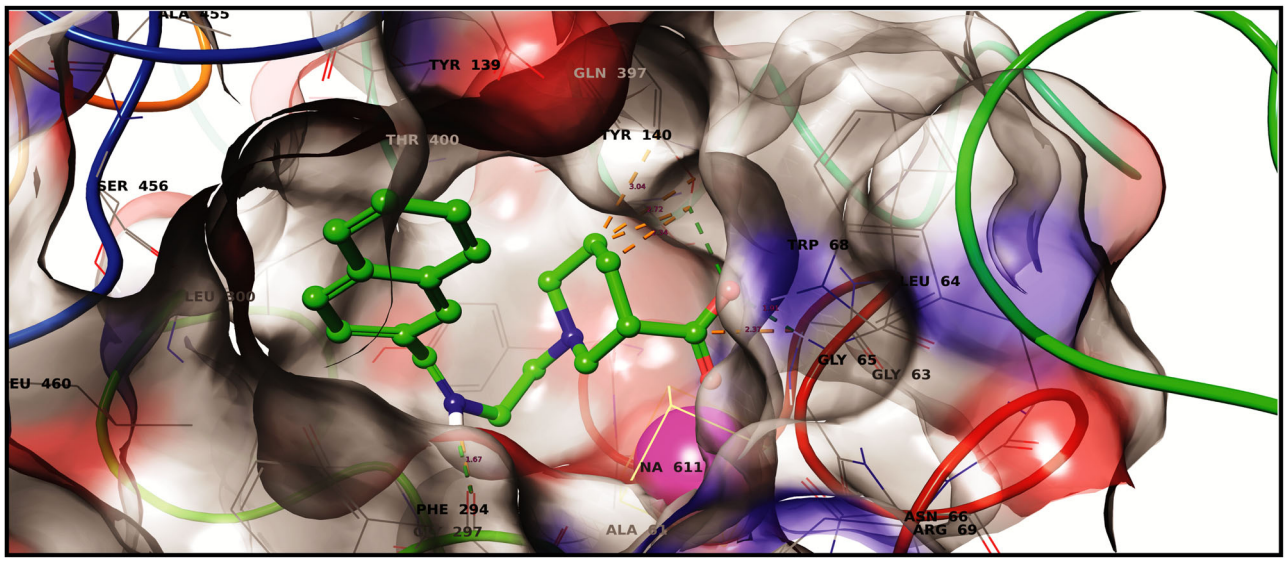

Fig. 4 3D Ribbon structure representation of docking conformation of the compound **5w** in the hydrophobic pocket of modeled protein structure of GAT1 GABA transporter (PDB Code: 4XP4). Structure of compound **5w** is shown as ball and stick model; light brown color surface showing hydrophobic pocket; the blue and red surface is charged surface of the protein; green dotted lines are H-bonding and orange dotted lines are Van der Waals interactions between active site amino acid residues and ligand

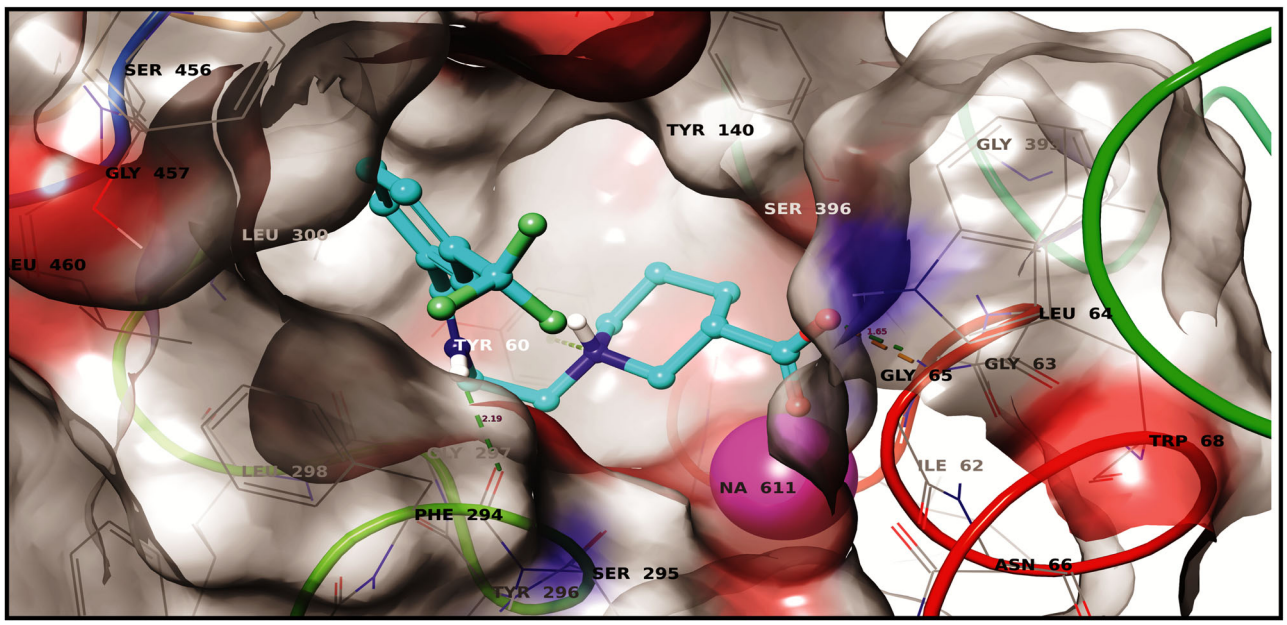

Fig. 5 3D Ribbon structure representation of docking conformation of the compound **5y** in the hydrophobic pocket of modeled protein structure of GAT1 GABA transporter (PDB Code: 4XP4). Structure of compound **5y** is shown as ball and stick model; light brown color surface showing hydrophobic pocket; the blue and red surface is charged surface of the protein; green dotted lines are H-bonding and orange dotted lines are Van der Waals interactions between active site amino acid residues and ligand

In silico prediction of "drug likeliness"

The results of some principle descriptors for the prediction of in silico "drug likeliness" of the most active compounds (**5d, 5w**, and **5y**) are mentioned in Table 7. The predicted values for QPlogBB and CNS activity predicted by QikProp method indicated that the selected compounds were found to be active for CNS and might be permeable across BBB. (Das et al. 2014) These results are comparable with the outcome of PAMPA-BBB assay and experimental log *P* values. However, the experimental log *P* values differ with that of the predicted values. The predicted PSA (polar surface area) values were found to be in the range of 58.378–59.856, which revealed that the selected

compounds showed lower polar surface area. Lower PSA is a key requisite for the compounds designed for CNS disorders.(Meena et al. 2015) The absence of reactive functional groups that causes decomposition, reactivity, or toxicity problems in vivo was predicted by the outcome of "rtvFG" value, which was found to be 0 for all the tested compounds. The test compounds demonstrated drug likeliness as per the Lipinski's rule of five (mol_MW < 500, QPlogPo/w < 5, donorHB ≤ 5, accptHB ≤ 10). QPlogKHSA values for the tested compounds fall within the limit, indicating considerable binding of the compounds with plasma proteins. Overall the predicted parameters revealed that the compounds **4a**, **4b**, and **4i** fulfill drug-like characteristics. (Banerjee et al. 2016)

Conclusion

In summary, we have successfully synthesized a series of novel *N*-substituted nipecotic acid derivatives following a synthetic approach of Schiff base formation through an ethylene bridge linker. Determination of brain permeability is very crucial for antiepileptic drugs to reach to the target site and elicit pharmacological activity. Amongst the synthesized compounds some potential leads have been identified with the ability to permeate the BBB by an in vitro PAMPA- BBB assay, mitigating the rationale of design. The permeability of the compounds **5d**, **5f**, **5j**, **5l**, **5m**, **5n**, **5w**, **5x**, and **5y** were comparable to tiagabine. The findings of in vivo PTZ, and DMCM induced rodent model epilepsy suggested that compounds **5d**, **5w**, **5y** were comparatively more active than **5d** and **5l**, while the compound **5n** was found inactive. Compounds **5d, 5w** and **5y** exhibited desirable physicochemical and drug-like properties. Based on the outcome of the in silico studies, we can reasonably infer that the potential derivatives inhibit GAT1 in a manner similar to tiagabine which may explain their underlying mechanism of action. Also the compounds **5d, 5w** and **5y** were found to be devoid of neurotoxicity as indicated by the results of MTT assay and rota rod test. Moreover the most active compound **5w** can be further quantified by in vitro GAT1 inhibitory/binding assay to provide a mechanistic pathway for anticonvulsant activity. All together the efficacy and safety of the potential leads justifies the rationale behind the study and provide a valuable insight towards the

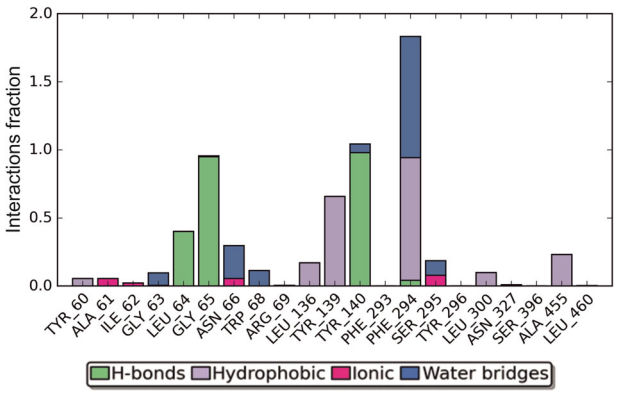

Fig. 7 Stacked bar charts of protein interactions with ligand **5w** as monitored throughout the MD simulation

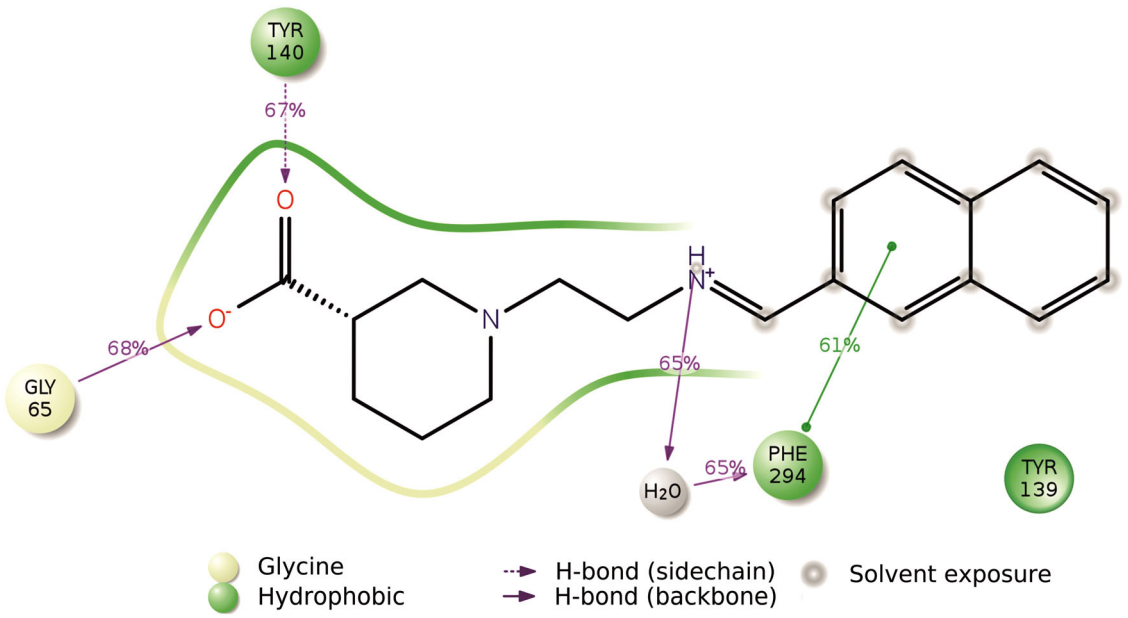

Fig. 6 The detailed atomic interactions of ligand **5w** with the key active amino acid residues with GABA GAT1 transporter protein of 4XP4

Table 7 In silico prediction of drug like properties of the active compounds **5d**, **5w**, **5y**

Comp.	Mol_MW (130–725)	QPlogBB (−3–1.2)	CNS (−2–+2)	QPlog *Po*/w (−2–6.8)	PSA (7-200)	QP log KHSA (−1.5–1.5)	Lipinski's rule of five (Max. 4)	donorHB (0–6)	accptHB (2–20)	#rtvFG (0–2)
5d	310.39	−0.267	0	1.579	59.856	0.053	0	1	5.5	0
5w	329.22	0.059	1	1.47	58.378	−0.106	0	1	5.5	0
5y	328.33	−0.005	0	1.625	59.195	−0.041	0	1	5.5	0

Mol_MW molecular weight, *QPlogBB* predicted brain/blood partition coefficient, *CNS* predicted central nervous system activity, *QPlogPo/w* predicted octanol/water partition coefficient, *PSA* polar surface area, *QPlogKHSA* prediction of binding to human serum albumin, *Rule of five* no. of violations of Lipinski's rule of five, *donorHB* No. of hydrogen bonds that would be donated by the solute to water molecules in an aqueous solution, *accptHB* No. of hydrogen bonds that would be accepted by the solute from water molecules in an aqueous solution, *#rtvFG* number of reactive functional group

development and optimization more promising compounds with superior anticonvulsant effects.

Compliance with ethical standards

Conflict of interest The authors declare that they have no conflict of interest.

References

Ali FE, Bondinell WE, Dandridge PA, Frazee JS, Garvey E, Girard GR, Kaiser C, Ku TW, Lafferty JJ, Moonsammy GI (1985) Orally active and potent inhibitors of gamma-aminobutyric acid uptake. J Med Chem 28:653–660

Aly MM, Mohamed YA, El-Bayouki KA, Basyouni WM, Abbas SY (2010) Synthesis of some new 4 (3H)-quinazolinone-2-carboxaldehyde thiosemicarbazones and their metal complexes and a study on their anticonvulsant, analgesic, cytotoxic and antimicrobial activities–Part-1. Eur J Med Chem 45:3365–3373

Ambrósio AF, Silva AP, Araújo I, Malva JO, Soares-da-Silva Pc, Carvalho AP, Carvalho CM (2000) Neurotoxic/neuroprotective profile of carbamazepine, oxcarbazepine and two new putative antiepileptic drugs, BIA 2-093 and BIA 2-024. Eur J Pharmacol 406:191–201

Andersen KE, Lau J, Lundt BF, Petersen H, Huusfeldt PO, Suzdak PD, Swedberg MD (2001a) Synthesis of novel GABA uptake inhibitors. Part 6: preparation and evaluation of N-Ω asymmetrically substituted nipecotic acid derivatives. Bioorg Med Chem 9:2773–2785

Andersen KE, Sørensen JL, Lau J, Lundt BF, Petersen H, Huusfeldt PO, Suzdak PD, Swedberg MD (2001b) Synthesis of novel γ-aminobutyric acid (GABA) uptake inhibitors. 5. 1 Preparation and structure− activity studies of tricyclic analogues of known GABA uptake inhibitors. J Med Chem 44:2152–2163

Araújo IM, Ambrósio AF, Leal EC, Verdasca MJ, Malva JO, Soares-da-Silva P, Carvalho AP, Carvalho CM (2004) Neurotoxicity induced by antiepileptic drugs in cultured hippocampal neurons: a comparative study between carbamazepine, oxcarbazepine, and two new putative antiepileptic drugs, BIA 2-024 and BIA 2-093. Epilepsia 45:1498–1505

Banerjee AG, Das N, Shengule SA, Sharma PA, Srivastava RS, Shrivastava SK (2016) Design, synthesis, evaluation and molecular modelling studies of some novel 5, 6-diphenyl-1, 2, 4-triazin-3 (2H)-ones bearing five-member heterocyclic moieties as potential COX-2 inhibitors: a hybrid pharmacophore approach. Bioorg Chem 69:102–120

Bhat MA, Al-Omar MA (2011) Synthesis, characterization and in vivo anticonvulsant and neurotoxicity screening of Schiff bases of phthalimide. Acta Pol Pharm 68:375–380

Bjorge S, Black A, Bockbrader H, Chang T, Gregor VE, Lobbestael SJ, Nugiel D, Pavia MR, Radulovic L, Woolf T (1990) Synthesis and metabolic profile of Cl-966: a potent, orally-active inhibitor of GABA uptake. Drug Dev Res 21:189–193

Braestrup C, Nielsen EB, Sonnewald U, Knutsen LJ, Andersen KE, Jansen JA, Frederiksen K, Andersen PH, Mortensen A, Suzdak PD (1990) R)-N-[4, 4-Bis (3-Methyl-2-Thienyl) but-3-en-1-yl] nipecotic acid binds with high affinity to the brain γ-aminobutyric acid uptake carrier. J Neurochem 54:639–647

Chen N-H, Reith ME, Quick MW (2004) Synaptic uptake and beyond: the sodium-and chloride-dependent neurotransmitter transporter family SLC6. Pflüg Arch 447:519–531

Das N, Garabadu D, Banerjee AG, Krishnamurthy S, Shrivastava SK (2014) Synthesis and pharmacological evaluation of some N3-aryl/heteroaryl-substituted 2-(2-chlorostyryl)-6, 7-dimethoxyquinazolin-4 (3H)-ones as potential anticonvulsant agents. Med Chem Res 23:4167–4176

Dhar TM, Borden LA, Tyagarajan S, Smith KE, Branchek TA, Weinshank RL, Gluchowski C (1994) Design, synthesis and evaluation of substituted triarylnipecotic acid derivatives as GABA uptake inhibitors: identification of a ligand with moderate affinity and selectivity for the cloned human GABA transporter GAT-3. J Med Chem 37:2334–2342

Di L, Kerns EH, Fan K, McConnell OJ, Carter GT (2003) High throughput artificial membrane permeability assay for blood–brain barrier. Eur J Med Chem 38:223–232

El-Helby AGA, Ayyad RR, Sakr HM, Abdelrahim AS, El-Adl K, Sherbiny FS, Eissa IH, Khalifa MM (2017) Design, synthesis, molecular modeling and biological evaluation of novel 2, 3-dihydrophthalazine-1, 4-dione derivatives as potential anticonvulsant agents. J Mol Struct 1130:333–351

Falch E, Krogsgaard-Larsen P (1989) GABA uptake inhibitors containing mono-and diarylmethoxyalkyl N-substituents. Drug Des Deliv 4:205–215

Gao X-M, Chuang D-M (1992) Carbamazepine-induced neurotoxicity and its prevention by NMDA in cultured cerebellar granule cells. Neurosci Lett 135:159–162

Gao X-M, Margolis RL, Leeds P, Hough C, Post RM, Chuang D-M (1995) Carbamazepine induction of apoptosis in cultured cerebellar neurons: effects ofN-methyl-d-aspartate, aurintricarboxylic acid and cycloheximide. Brain Res 703:63–71

Ghadimi S, Latif Mousavi S, Javani Z (2008) Synthesis, lipophilicity study and in vitro evaluation of some rodenticides as acetylcholinesterase reversible inhibitors. J Enzyme Inhib Med Chem 23:213–217

Ghareb N, Daim MMA, El-Sayed NM, Elgawish MS (2017) Synthesis, molecular modelling, and preliminary anticonvulsant activity evaluation of novel naphthalen-2-yl acetate and 1, 6-dithia-4, 9-diazaspiro [4.4] nonane-3, 8-dione derivatives. Bioorg Chem 71:110–119

Holmes GL (1995) Role of glutamate and GABA in the pathophysiology of epilepsy. Dev Disabil Res Rev 1:208–219
Jurik A, Reicherstorfer R, Zdrazil B, Ecker GF (2013) Classification of high-activity tiagabine analogs by binary QSAR modeling. Mol Inform 32:415–419
Jurik A, Zdrazil B, Holy M, Stockner T, Sitte HH, Ecker GF (2015) A binding mode hypothesis of tiagabine confirms liothyronine effect on γ-aminobutyric acid transporter 1 (GAT1). J Med Chem 58:2149–2158
Kälviäinen R (2001) Long-term safety of Tiagabine. Epilepsia 42:46–48
Kim M, Cho AE (2016) Incorporating QM and solvation into docking for applications to GPCR targets. Phys Chem Chem Phys 18:28281–28289
Kowalczyk P, Sałat K, Höfner GC, Mucha M, Rapacz A, Podkowa A, Filipek B, Wanner KT, Kulig K (2014) Synthesis, biological evaluation and structure–activity relationship of new GABA uptake inhibitors, derivatives of 4-aminobutanamides. Eur J Med Chem 83:256–273
Krogsgaard-Larsen P (1980) Inhibitors of the GABA uptake systems. Mol Cell Biochem 31:105–121
Krogsgaard-Larsen P, Johnston G (1975) Inhibition of GABA uptake in rat brain slices by nipecotic acid, various isoxazoles and related compounds. J Neurochem 25:797–802
Kulkarni A, Wankhede S, Dhawale N, Yadav P, Deore V, Gonjari I (2017) Synthesis, characterization and biological behavior of some Schiff's and Mannich base derivatives of Lamotrigine. Arab J Chem 10:S184–S189
Lim S-W, Loh H-S, Ting K-N, Bradshaw TD, Allaudin ZN (2015) Reduction of MTT to purple formazan by vitamin E isomers in the absence of cells. Trop Life Sci Res 26:111
Liu Y, Wang X-y, Li D, Yang L, Huang S-p (2015) Short-term use of antiepileptic drugs is neurotoxic to the immature brain. Neural Regen Res 10:599
Löscher W (1985) Anticonvulsant action in the epileptic gerbil of novel inhibitors of GABA uptake. Eur J Pharmacol 110:103–108
Meena P, Nemaysh V, Khatri M, Manral A, Luthra PM, Tiwari M (2015) Synthesis, biological evaluation and molecular docking study of novel piperidine and piperazine derivatives as multi-targeted agents to treat Alzheimer's disease. Bioorg Med Chem 23:1135–1148
Murali Dhar T, Nagarathnam D, Marzabadi MR, Lagu B, Wong WC, Chiu G, Tyagarajan S, Miao SW, Zhang F, Sun W (1999) Design and synthesis of novel α1a adrenoceptor-selective antagonists. 2. Approaches to eliminate opioid agonist metabolites via modification of linker and 4-methoxycarbonyl-4-phenylpiperidine moiety. J Med Chem 42:4778–4793
Nielsen EB, Suzdak PD, Andersen KE, Knutsen LJ, Sonnewald U, Braestrup C (1991) Characterization of tiagabine (NO-328), a new potent and selective GABA uptake inhibitor. Eur J Pharmacol 196:257–266
Nonaka S, Katsube N, Chuang D-M (1998) Lithium protects rat cerebellar granule cells against apoptosis induced by anticonvulsants, phenytoin and carbamazepine. J Pharmacol Exp Ther 286:539–547
Ortinski P, Meador KJ (2004) Cognitive side effects of antiepileptic drugs. Epilepsy Behav 5:60–65
Pandeya SN, Rajput N (2012) Synthesis and anticonvulsant activity of various Mannich and Schiff bases of 1,5-benzodiazepines. Int J Med Chem 2012:1–10
Pavia MR, Lobbestael SJ, Nugiel D, Mayhugh DR, Gregor VE, Taylor CP, Schwarz RD, Brahce L, Vartanian MG (1992) Structure-activity studies on benzhydrol-containing nipecotic acid and guvacine derivatives as potent, orally-active inhibitors of GABA uptake. J Med Chem 35:4238–4248
Petersen EN (1983) DMCM: a potent convulsive benzodiazepine receptor ligand. Eur J Pharmacol 94:117–124
Petrera M, Wein T, Allmendinger L, Sindelar M, Pabel J, Höfner G, Wanner KT (2016) Development of highly potent GAT1 inhibitors: synthesis of nipecotic acid derivatives by Suzuki–Miyaura cross-coupling reactions. ChemMedChem 11:519–538
Petroff OA, Rothman DL, Behar KL, Mattson RH (1996) Low brain GABA level is associated with poor seizure control. Ann Neurol 40:908–911
Prescott L (1997) Tiagabine offers effective seizure control. Inpharma Wkly 1085:15–16
Quandt G, Höfner G, Wanner KT (2013) Synthesis and evaluation of N-substituted nipecotic acid derivatives with an unsymmetrical bis-aromatic residue attached to a vinyl ether spacer as potential GABA uptake inhibitors. Bioorg Med Chem 21:3363–3378
Regulska M, Pomierny B, Basta-Kaim A, Starek A, Filip M, Lasoń W, Budziszewska B (2010) Effects of ethylene glycol ethers on cell viability in the human neuroblastoma SH-SY5Y cell line. Pharmacol Rep 62:1243–1249
Shidore M, Machhi J, Shingala K, Murumkar P, Sharma MK, Agrawal N, Tripathi A, Parikh Z, Pillai P, Yadav MR (2016) Benzylpiperidine-linked Diarylthiazoles as potential anti-Alzheimer's agents: synthesis and biological evaluation. J Med Chem 59:5823–5846
Siddiqui N, Alam MS, Sahu M, Naim MJ, Yar MS, Alam O (2017) Design, synthesis, anticonvulsant evaluation and docking study of 2-[(6-substituted benzo [d] thiazol-2-ylcarbamoyl) methyl]-1-(4-substituted phenyl) isothioureas. Bioorg Chem 71:230–243
Singh RB, Singh GK, Chaturvedi K, Kumar D, Singh SK, Zaman MK (2017) Design, synthesis, characterization, and molecular modeling studies of novel oxadiazole derivatives of nipecotic acid as potential anticonvulsant and antidepressant agents. Med Chem Res 27:137–152
Skovstrup S, Taboureau O, Bräuner-Osborne H, Jørgensen FS (2010) Homology modelling of the GABA transporter and analysis of tiagabine binding. ChemMedChem 5:986–1000
Suzdak PD, Jansen JA (1995) A review of the preclinical pharmacology of tiagabine: a potent and selective anticonvulsant GABA uptake inhibitor. Epilepsia 36:612–626
Sveinbjornsdottir S, Sander J, Patsalos P, Upton D, Thompson P, Duncan J (1994) Neuropsychological effects of tiagabine, a potential new antiepileptic drug. Seizure 3:29–35
Swathi K, Sarangapani M (2015) Synthesis and antiepileptic activity of Schiff's bases of dialkylamino alkoxy isatin derivatives. GeNeDis 2014. Springer International Publishing, Swizerland
Taylor CP, Vartanian MG, Schwarz RD, Rock DM, Callahan MJ, Davis MD (1990) Pharmacology of Cl-966: A potent GABA uptake inhibitor, in vitro and in experimental animals. Drug Dev Res 21:195–215
Thompson SM, Gahwiler B (1992) Effects of the GABA uptake inhibitor tiagabine on inhibitory synaptic potentials in rat hippocampal slice cultures. J Neurophysiol 67:1698–1701
Villalba ML, Enrique AV, Higgs J, Castaño RA, Goicoechea S, Taborda FD, Gavernet L, Lick ID, Marder M, Blanch LEB (2016) Novel sulfamides and sulfamates derived from amino esters: synthetic studies and anticonvulsant activity. Eur J Pharmacol 774:55–63
Wang KH, Penmatsa A, Gouaux E (2015) Neurotransmitter and psychostimulant recognition by the dopamine transporter. Nature 521:322–327
Yunger L, Fowler P, Zarevics P, Setler P (1984) Novel inhibitors of gamma-aminobutyric acid (GABA) uptake: anticonvulsant actions in rats and mice. J Pharmacol Exp Ther 228:109–115